ORIGINAL ARTICLE

Phylogenetic relationships in Stephanopinae: systematics of *Stephanopis* and *Sidymella* based on morphological characters (Araneae: Thomisidae)

Miguel Machado[1] · Renato Augusto Teixeira[1]

Abstract

A matrix of 117 morphological characters scored for 77 terminal taxa was subjected to parsimony analysis under equal and implied weighting schemes and to Bayesian inference in order to test the relationships in and between *Stephanopis* and *Sidymella* species, as well as its implications for the systematics of the subfamily Stephanopinae. A sensitivity test was performed to evaluate nodal stability. Our results indicate the polyphyletism of both genera and the topologies obtained allowed the proposition of the following taxonomic acts: The "*altifrons* clade" is the only group considered as *Stephanopis* (stricto sensu), with species restricted to the Australian region; most species from the Neotropical region, hitherto attributed to this genus, formed the well-supported "*pentacantha* clade", while two of them, restricted to Central America, were recovered as the "*championi* clade". The latter shows significative evidences for the revalidation of *Paratobias* **gen. rev**.; the "*cambridgei* clade" emerged with *I. punctata* nested within, having all its component species transferred to *Isala*. None of the *Sidymella* species with Australian distribution seems to be part of this genus, which occurs in fact only in the Neotropical region and is closely related to *Coenypha*. This latter has an increment of three species transferred from *Stephanopis*. Aside from the "*lucida* clade", which is considered here as *Sidymella* (stricto sensu), three other groups and a single species emerged apart from this genus: the "*hirsuta* clade", "*trapezia* clade", "*angularis* clade" and *Si. rubrosignata*. Morphological evidences seem to justify the proposition of all these groups as new genera.

Keywords Australian · Cladistic · Neotropical · Spider · Systematics

Introduction

The subfamily Stephanopinae has been the focus of recent revisional works (Benjamin 2013, 2015, 2016, 2017; Machado et al. 2015, 2017, 2018, 2019a, b; Silva-Moreira and Machado 2016; Prado et al. 2018). Even so, most of its component genera are still poorly known and diagnosed, which is reflected in the lack of resolution and constant recovery of its polyphyletic relations (Benjamin et al. 2008; Benjamin 2011; Wheeler et al. 2017). The genus that gives name to the subfamily had its Australian species recently revised by Machado et al. (2019b), but despite the recent efforts to better understand the morphology of *Stephanopis* O. Pickard-Cambridge, 1869, our knowledge regarding the Neotropical and Andean species of the genus relies only on original descriptions. A similar scenario is observed for *Sidymella* Strand, 1942, which also had its diagnosis and description updated by Machado et al. (2019a). However, in this case, only the Neotropical species were considered in the taxonomic work while the Australian ones remain in need of revision.

The distribution regions of both *Stephanopis* and *Sidymella* overlap, occurring along the Neotropical and Australian regions (World Spider Catalog 2020). Some species present striking morphological similarities and crossed taxonomic backgrounds. Descriptions of wrongly assigned species also highlight their blurred taxonomic limits. Simon (1895) already mentioned that *Stephanopis* was barely homogenous, pointing out some notable differences between its Australian (i.e.,

✉ Miguel Machado
machadom.arachno@gmail.com

1   Laboratório de Aracnologia, Escola de Ciências da Saúde e da Vida, Pontifícia Universidade Católica do Rio Grande do Sul (PUCRS), Porto Alegre, Rio Grande do Sul, Brazil

Stephanopis altifrons O. Pickard-Cambridge, 1869*; Stephanopis scabra* L. Koch, 1874*; Stephanopis cambridgei* Thorell, 1870) and South American species (i.e. *Stephanopis ditissima* (Nicolet, 1874)), especially regarding the length and height of their prosoma as well as the shape of their abdominal projections. According to this author, there were four distinguishable groups within *Stephanopis* (represented by *St. altifrons*, *St. ditissima*, *Stephanopis bicornis* L. Koch, 1874 and *Sidymella rubrosignata* (L. Koch, 1874)—the latter previously assigned to *Stephanopis*), which made him question the validity of the genus. While Simon (1895) considered Australian and Neotropical representatives of *Stephanopis* to make this statement, Machado et al. (2019b), based on comparisons of both somatic and sexual traits, inferred the existence of three different groups within a group of species with distribution ranges restricted to Australia, Indonesia, Papua New Guinea and Fiji, called them "*cambridgei* group", "*lata* group" and "*altifrons* group".

The genus *Stephanopis* comprises 47 species, was originally proposed based on a female of *St. altifrons* and is currently characterized by their high clypeus, cephalic prominence, dorsoventrally depressed prosoma, robust legs with dorsal acute projections and remarkable setiferous tubercles along their patellae and tibiae (Machado et al. 2019b). Despite the recent taxonomic review and updated diagnosis, the validity of the genus remains uncertain. Unlike what is presented in current morphological studies on spiders, genitalic features were not always considered in classic taxonomic works. The most common characteristics considered by earlier naturalists to assign a given species to *Stephanopis* were general somatic features related to the cryptic habitus of the spiders (e.g. Simon 1895; Pickard-Cambridge1869; Bradley 1871; Koch 1874; Mello-Leitão 1929). Both the Australian and Neotropical species of *Stephanopis* indeed share characteristics of a typical bark-dwelling stephanopine, as pointed out by Machado et al. (2017), such as rugose tegument and predominantly dark body coloration. Additionally, many species bear soil particles attached to their tegument or present some association with lichens and/or fungi (Ramirez 2014). Nevertheless, it is still unknown if this set of features is the result of an evolutionary convergence related to hunt/camouflage adaptations or if *Stephanopis* is indeed monophyletic. The same question deserves a proper study in regard to the bifid opisthosoma of *Sidymella* species, a trait that was still recently considered by Machado et al. (2019a) as one of the main traits to diagnose the genus.

The genus *Sidymella*, described based on *Sidymella lucida* (Keyserling, 1880), is currently recognized by males having a long, thin and curled embolus, well-developed pars pendulum and retrolateral tibial apophysis with a short basal branch (Machado et al. 2019a). Females present a median septum on the epigynal plate, long and coiled copulatory ducts and compartmentalized spermathecae with accessory glands (Machado et al. 2019a). Despite sharing the presence of the posterior pair of lateral projections on the opisthosoma, other somatic characteristics observed in Australian representatives of the genus are not comprehended by the diagnosis and descriptions provided by Machado et al. (2019b). Moreover, the genitalic features mentioned above differ from what Koch (1874) described for *Sidymella bicuspidata* (L. Koch, 1874), *Sidymella hirsuta* (L. Koch, 1874), *Sidymella lobata* (L. Koch, 1874), *Sidymella longipes* (L. Koch, 1874), *Si. rubrosignata* and *Sidymella trapezia* (L. Koch, 1874). Therefore, a broader study must be carried out to check such incongruences.

Considering these previous observations and insights, in the current study, we perform a phylogenetic analysis based on an extensive morphological dataset that aims to test the monophyly and relationships in and between *Stephanopis* and *Sidymella*.

Materials and methods

Cladistic analysis

The character matrix (Electronic supplementary material 1) was assembled in Mesquite 3.51 (Maddison and Maddison 2019) starting from preliminary results published by Machado et al. (2017), from where most of the characters were adapted. We also incorporated propositions made by Benjamin (2011) and Ramírez (2014) into our dataset. Aiming to explore different perspectives of reconstruction of the evolutionary relationships, two optimality criteria were chosen: Bayesian inference (BI) and maximum parsimony (MP). In spite of recent discussions regarding which would be the best method to infer phylogenies based on morphological characters (Goloboff et al. 2008b; O'Reilly et al. 2018; Goloboff et al. 2018a, b; Puttick et al. 2019), some authors such as Smith (2019) show that both approaches are likely to be equally informative. In compliance with the proposition made by this author, we chose to perform analyses using both methods, comparing the results to find the most congruent and supported clades. Poorly resolved topologies were submitted to search routines where taxa with variable placement in the topology (wild cards) were pruned from the tree. Pruning was applied only when the absence of a clade provided more gains in resolution (resolved nodes) than removed terminals.

The Bayesian inference was performed in MrBayes 3.2.0 (Ronquist et al. 2012). The parameters were the same as those considered by Ronquist et al. (2012) as appropriate to the kind of data these authors called "standard". The routines used were as follows: (1) set the Mk model [lset nst=1 rates=equal]; (2) set MCMC generation parameter [mcmcp ngen=5000000 relburnin=no printfreq=1000 samplefreq=1000 nchains=4 savebrlens=yes]; (3) run the analysis [mcmc]. After that, the

stationary distribution of the chains was recovered with Tracer v.1.6.0 (Rambaut et al. 2018) and used to burn-in the first 10% of the generations. The remaining generations were used to estimate the posterior probability in a majority consensus tree.

Heuristic searches for most-parsimonious trees were made in TNT 1.1 (Goloboff et al. 2008a). Under maximum parsimony, the dataset was submitted to two different analyses: (1) equal weighting (EW) and (2) implied weighting (IW). For the latter, we followed the methodology described by Mirande (2009), which attributes several *K* values to a symmetric variation of the mean fit that each extra step represents in relation to a transformation. The values for concavity indices were calculated in a way that each extra step represent *X*% of the value of the previous transformation. Thus, we assigned 16 distortion values to "*X*" ranging from 50 to 90% of fitting. The parameters used in this weighting regime were the same as those by Machado et al. (2017). Seeking to create a simplified batch of search routines, we followed the tutorial provided by Weiler et al. (2016) to calculate the parameters manually (Electronic supplementary material 2— 'stephanopisroutine.run'). The following commands were set for analyses of MP (commands in TNT are shown in brackets): (1) memory was set to keep up to 500,000 trees [hold500000]; (2) search started from a random tree [rseed*]; (3) ratchet was set to perturb up to 5% of the characters, both down and up and to do 10 cycles of auto-constrains [rat:equal upfac5 downfac5 autoconst10]; (4) rearrangements were performed by random addition sequence (RAS) using tree bisection and reconnection (TBR) in cycles of sectorial searches (including default parameters of consensus-based and random rearrangement), 100 iterations of ratchet and 2 of tree fusing (Nixon 1999; Goloboff 1999) [xmult:ras css rss rat100 fuse2]; (5) rearrangement cycles were repeated 10 times until the most parsimonious result was obtained twice [xmult: hit2 rep10]; (6) finally, the obtained results were submitted to a new TBR turn with branch-swap [bb]. The strict consensus was saved and posteriorly edited in WinClada-Asado ver. 1.89 (Nixon 1999-2004), where the characters were optimized. Branch supports were estimated through relative Bremer support (Goloboff and Farris 2001) and symmetric resampling (Goloboff et al. 2003) in a similar manner to that of the abovementioned routine (Electronic supplementary material 3— 'stephanopisSUP.run').

Although all resulting trees should be seen as plausible results to be considered as hypothetical topologies, the "best" tree must represent the more stable taxonomic lineages and trees with highest supports. Since all our analyses presented low values for branch supports, we searched for clades with high stability to be represented and therefore discussed. Thus, we compared pairs of trees counting how many SPR movements (pruning a subtree and rearranging it by its root to the edge of the resulting tree) were required to make both topologies identical, converting such movements into a similarity index (Teixeira et al. 2014) (see electronic supplementary material 4– sprdf.run). The best phylogenetic reconstruction was the one whose tree had the greatest sum of similarities with every other consensus trees from the rest of the analytical conditions, being considered the most congruent (Electronic supplementary material 5– 'IW values and SPR comparisons'). The consensus of all trees, including BI and both EW and IW for MP, was summarized on the "best/most congruent" tree in a sensitivity analysis performed in the software Ybyrá (Machado 2015).

Choice of terminal taxa and examined species

Recent studies suggest that Stephanopinae is not monophyletic once none of its proposed diagnostic features had been recovered as reliable morphological synapomorphies (Benjamin et al. 2008; Benjamin 2011; Ramirez 2014; Wheeler et al. 2017). Consequentially, most of its component genera behave unpredictably in phylogenies, presenting poorly supported and unclear relationships. In light of this issue, and seeking to avoid problems regarding character polarization, we included as many Stephanopinae genera as possible in our data matrix. Two species of *Tmarus* Simon, 1875 were also scored to verify the placement of the "*Thomisus* clade" (sensu Benjamin et al. 2008). The tree was rooted in *Borboropactus nyerere* Benjamin, 2011 once *Borboropactus* Simon, 1884 is considered to be sister to all other Thomisidae genera (Wheeler et al. 2017).

The ingroup includes 31 of the 47 valid species of *Stephanopis*, and 13 of the 20 species currently assigned as *Sidymella*. Species known only by their type material or examined through photographs were not scored, as handling the specimens or SEM preparations and detailed observation of microstructures were not possible. All Australian representatives of *Stephanopis* were included in the matrix, while the Neotropical diversity of the genus was partially sampled. This was deliberately done because the taxonomic review of Australian species was recently published (Machado et al. 2019b), while the Neotropical species remain in need of revision. Nevertheless, as we are currently working on the morphological delimitation of the Neotropical species, we refrained from including different names that are undoubtedly synonyms of those already shown here, avoiding scoring the same species twice. Similarly, the recently revised *Sidymella* species from the Neotropical region (Machado et al. 2019a) were all included, whereas Australian species that were identified as junior synonyms or *nomina dubia* were not scored. Three undescribed species were also added to test their placement in the phylogeny.

We followed Morrone (2014, 2015) in considering the regionalization of the Neotropical ecozone and Andean region, respectively. In this way, we refer to distinct clades of the ingroup according to their geographic distribution. (e.g. "Australian *Stephanopis*", "Neotropical *Stephanopis*", "Australian *Sidymella*" and "Neotropical *Sidymella*").

Despite a considerable part of the Andes Mountain Range being outside of the Andean region, the term "Andean *Stephanopis*" is used to objectively refer to the group of species of this genus which are recorded along the Subantarctic and Patagonian regions (sensu Morrone (1994)).

The specimens examined (Appendix 1) are deposited in the following institutions (acronyms and curators in parentheses): Australian Museum, Sydney, Australia (AMS, Graham Milledge); California Academy of Sciences, San Francisco, USA (CAS, Lauren Esposito); Instituto Butantan, São Paulo, Brazil (IBSP, Antonio D. Brescovit); Instituto Nacional de Pesquisas da Amazônia, Manaus, Brazil (INPA, L. R. França); Museo Nacional de Historia Natural, Santiago, Chile (MNHN, Andrea Martínez); Museu de Ciências e Tecnologia da Pontifícia Universidade Católica do Rio Grande do Sul, Porto Alegre, Brazil (MCTP, Renato A. Teixeira); Museu de Ciências Naturais da Fundação Zoobotânica do Rio Grande do Sul, Brazil (MCN, Ricardo Ott); Museu Nacional do Rio de Janeiro, Brazil (MNRJ, Adriano B. Kury); Museu Paraense Emílio Goeldi, Belém, Brazil (MPEG, Alexandre B. Bonaldo); Museum für Naturkunde der Humboldt-Universität, Berlin, Germany (ZMB, Jason Dunlop); Museum National d'Histoire Naturelle, Paris, France (MNHN, Christine Rollard); Museum of Comparative Zoology of Harvard, Cambridge, USA (MCZ, Gonzalo Giribet and Laura Liebensperger); Oxford University Museum of Natural History, Oxford, UK (OUMNH, Zoë M. Simmons); Queensland Museum, Brisbane, Australia (QM, Robert Raven) and Universidade Federal de Minas Gerais, Belo Horizonte, Brazil (UFMG, Adalberto J. Santos).

Laboratory procedures and specimen preparation

The terminology used to name both somatic and copulatory structures follows that of Machado et al. (2018). The female genitalia were detached and submerged in pancreatin solution in a double boiler for a few minutes. The slight and gradual increase in temperature provided total digestion of the soft tissues without risking the integrity of the delicate diagnostic structures. Males had their left palpus removed and represented in ventral and retrolateral views. Palpi were not submerged in KOH because in Thomisidae the compact tegulum allows the observation of all structures (e.g. apophysis, embolus, tegular ridge) in the ventral view without the need for expansion processes. The material was observed under a stereomicroscope model Zeiss®Stemi SV6. Photographs of the dorsal habitus, front and both male and female genitalia were taken on a Multipurpose Zoom Microscope Leica M205A with a digital camera, and scanning electron microscopy was conducted with a Philips XL 30 from the Centro de Microscopia e Microanálises (CEMM) of the Pontifícia Universidade Católica do Rio Grande do Sul (PUCRS).

The anatomical abbreviations used in this study are as follows: AH, anterior hood; ALE, anterior lateral eye; AME, anterior median eye; CD, copulatory duct; CO, copulatory opening; EpT, epyginal teeth; S, spermathecae; MSept, median septum; MS, median spire; PLE, posterior lateral eye; PME, posterior median eye; RTA, retrolateral tibial apophysis; RTAvbr, retrolateral tibial apophysis' ventral branch; VTA, ventral tibial apophysis; Em, embolus; CP, cymbial process; T, tegulum; PrsP, pars pendulum; C, conductor; MA, median apophysis; TR, tegular ridge.

Results

The 117 morphological characters (Appendix 2) of our final dataset were scored for both sexes in 58 of the 77 terminal taxa. Six species were represented only by males and 13 only by females. Seventy percent of the entries were composed of somatic features while male genitalia represented 20.5% of the analysed data and the epigyna represented 9.5% of the characters (Electronic supplementary material 1).

Equal weight analysis found 288 most parsimonious trees with 734 steps, consistency index (CI) = 0.20 and retention index (RI) = 0.70. The strict consensus shows a lack of resolution among the outgroup species and for basal branches in general; however, more distal clades were better resolved (Fig. 1). Implied weight analysis of 16 distortion groups subjected to similarity comparisons (sprdiff command) showed three most-congruent trees with identical topologies (Electronic supplementary material 5– 'IW values and SPR comparisons'). The most parsimonious tree obtained under K = 17.89 (fit = 23.209) is used as a hypothetical reconstruction to discuss character transformations and the relationships in the ingroup (Fig. 2). The topology obtained through Bayesian inference had 96% of similarity when compared to equal weight parsimony (Fig. 1) and 85% when compared to the preferred tree under implied weighting (K = 17.89) (Electronic supplementary material 5– 'IW values and SPR comparisons'). Regardless of how homoplasies were treated (equal or implied weight), most deep relationships were weakly supported, and both *Stephanopis* and *Sidymella* were shown to be polyphyletic under any optimality criteria (Figs. 1 and 3).

The polyphyletic relations in *Stephanopis* showed species emerging in five distinct clades (Fig. 3). The genus *Coenypha* Simon, 1895 was nested within the "Andean *Stephanopis*", being this clade recovered as sister group to "Neotropical *Sidymella*". The "Australian *Stephanopis*", on the other hand, emerged in two major clades: one is composed of the "*altifrons* group" + "*lata* group" (sensu Machado et al. (2019b)), and the other is formed by all species of the "*cambridgei* group" (*sensu* Machado et al. (2019b)) with *Isala punctacta* L. Koch, 1876 nested within. Most "Neotropical *Stephanopis*" emerged as sister to *Rejanellus*
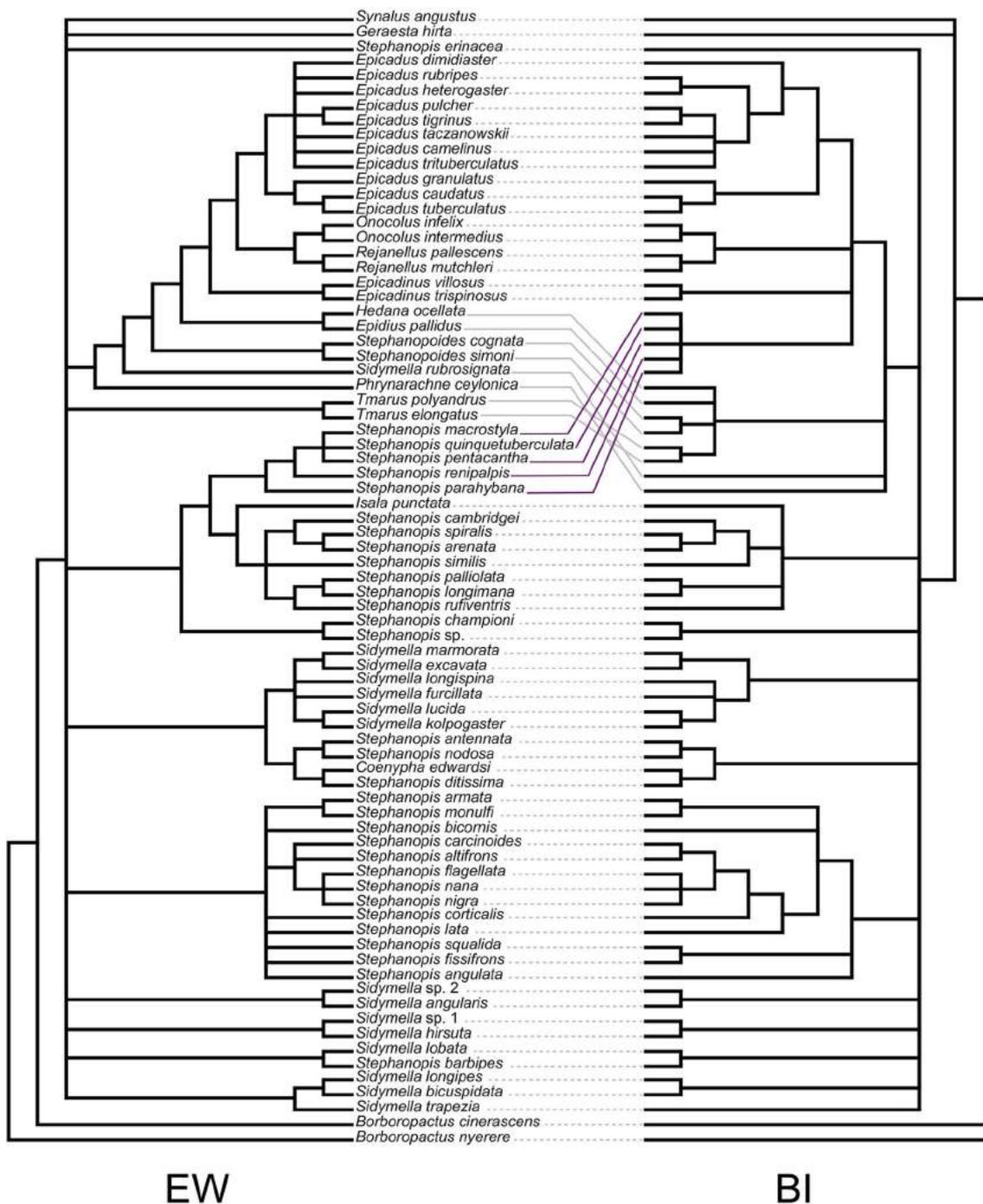
Fig. 1 Topologic comparison between consensuses trees obtained under equal weighting parsimony (EW) and Bayesian inference (BI)

Lise, 2005, integrating the "*Epicadus* group" (sensu Silva-Moreira and Machado (2016)). While this clade is composed by species recorded for the Amazon Rainforest, Atlantic Forest and Cerrado biomes, the species with distribution restricted to Central America *Stephanopis championi* (F. O. Pickard-Cambridge, 1900) and *Stephanopis* sp. 1 were recovered in a dichotomy with species of the "*cambridgei* group" (sensu Machado et al. (2019b)).

The species of *Sidymella* emerged as polyphyletic, arranged in three distinct clades (Fig. 3). All "Neotropical *Sidymella*" emerged in a single clade related to *Coenypha* + "Andean *Stephanopis*". The Australian representatives of the genus, on the other hand, were split into four distinct groups, which were relatively well supported by resampling analysis and Bremer support values, except the "*trapezia* clade".

File name	Distortion	K
k0	0.90	35.34
k1	0.87	27.07
k2	0.85	21.68
k3	**0.82**	**17.89**
k4	0.79	15.07
k5	0.77	12.90
k6	0.74	11.17
k7	0.71	9.77
k8	0.69	8.60
k9	0.66	7.62
k10	0.63	6.78
k11	0.61	6.06
k12	0.58	5.42
k13	0.55	4.86
k14	0.53	4.37
k15	0.50	3.93

k0	k1	k2	k4	k5
k6	k7	k8	k9	k10
k11	k12	k13	k14	k15
EW			BI	
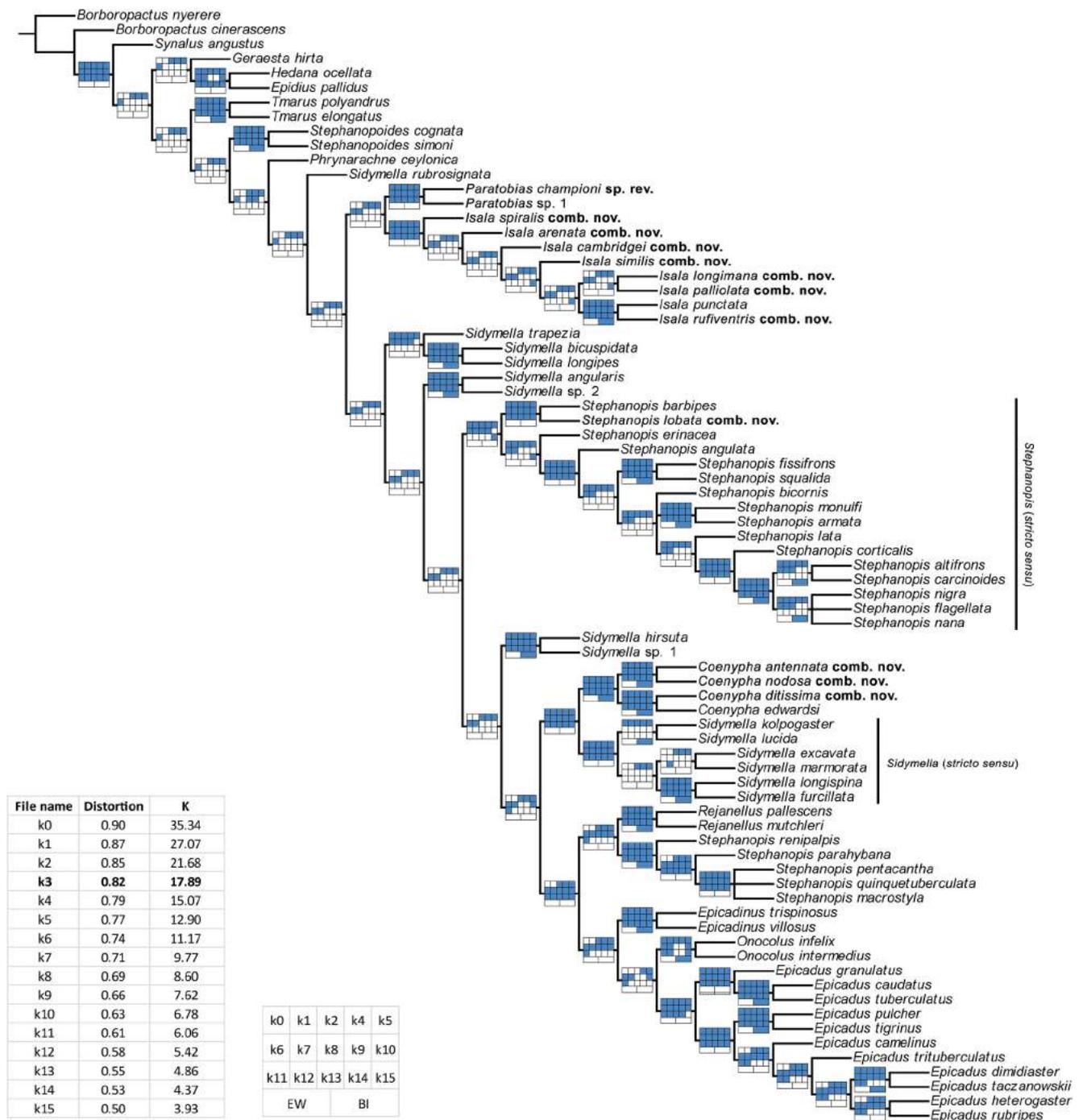
Fig. 2 Hypothetical reconstruction of the relationships of *Stephanopis* and *Sidymella* based on the strict consensus of the most congruent tree (K = 17.89) obtained after implied weighted analysis. Nodal stability is represented by the "Navajo rugs" along the branches (analysis recovering the clades as shown in the discussed topology are represented by blue squares while alternative resolutions are those in white). EW, equal weight; BI, Bayesian inference

Discussion

Recent phylogenetic works on spiders have been frequently showing weakly supported and unstable relationships among stephanopines (Benjamin 2011; Ramírez 2014; Wheeler et al. 2017). As noted by Benjamin et al. (2008), most genera in this subfamily, especially from the Australian and Neotropical regions, are not monophyletic. Benjamin (2011) highlights that, in these regions, there is a considerable number of species yet to be described and that most genera are in need of taxonomic revisions. This author states that these might be good reasons that can explain the instability and lack of support for
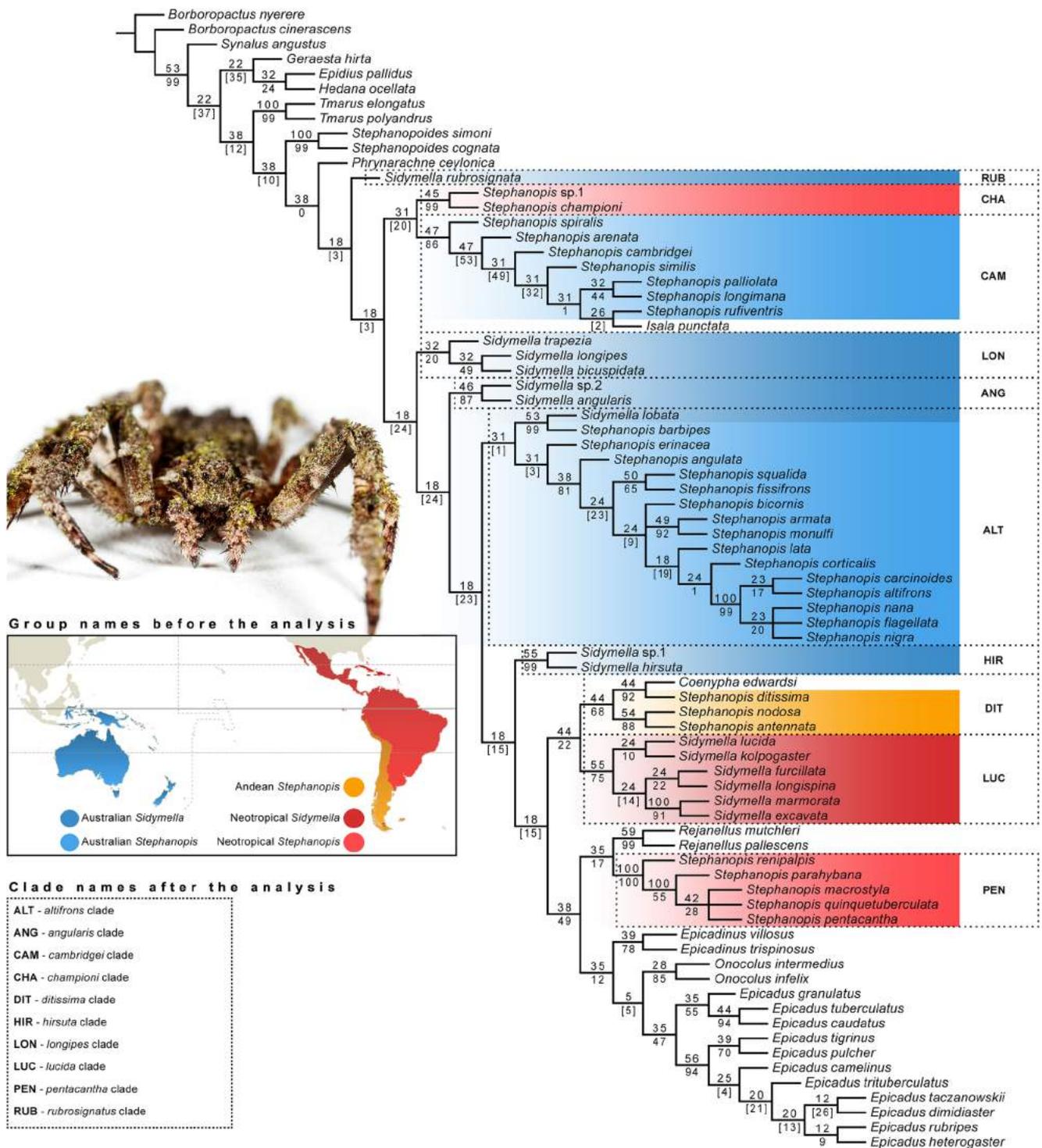
Fig. 3 Clade supports obtained by relative Bremer index (above the branches) and symmetric resampling analysis (below the branches). A colour scheme is applied to represent the geographical distribution of the clades represented on the working phylogenetic hypothesis

these thomisid groups in phylogenetic works, which seems to be applicable to both genera studied here.

The presence of rugose tegument (char. 1, state 1; see Fig. 4a), considered by Simon (1895) as a diagnostic feature of *Stephanopis*, was also found in *Epicadinus* Simon, 1895, *Onocolus* Simon, 1895, *Phrynarachne* Thorell, 1869,

Rejanellus, *Isala* L. Koch, 1876, *Epicadus* Simon, 1895, *Coenypha*, *Si. bicuspidata*, *Sidymella angularis* (Urquhart, 1885), and *Geraesta* Simon, 1889. The cryptic behaviour through adhesion of lichen or soil particles (char. 3, state 1; see Fig. 4f), another diagnostic feature of the genus, was coded as present for *Borboropactus*, *Synalus* Simon, 1895, *Isala*,
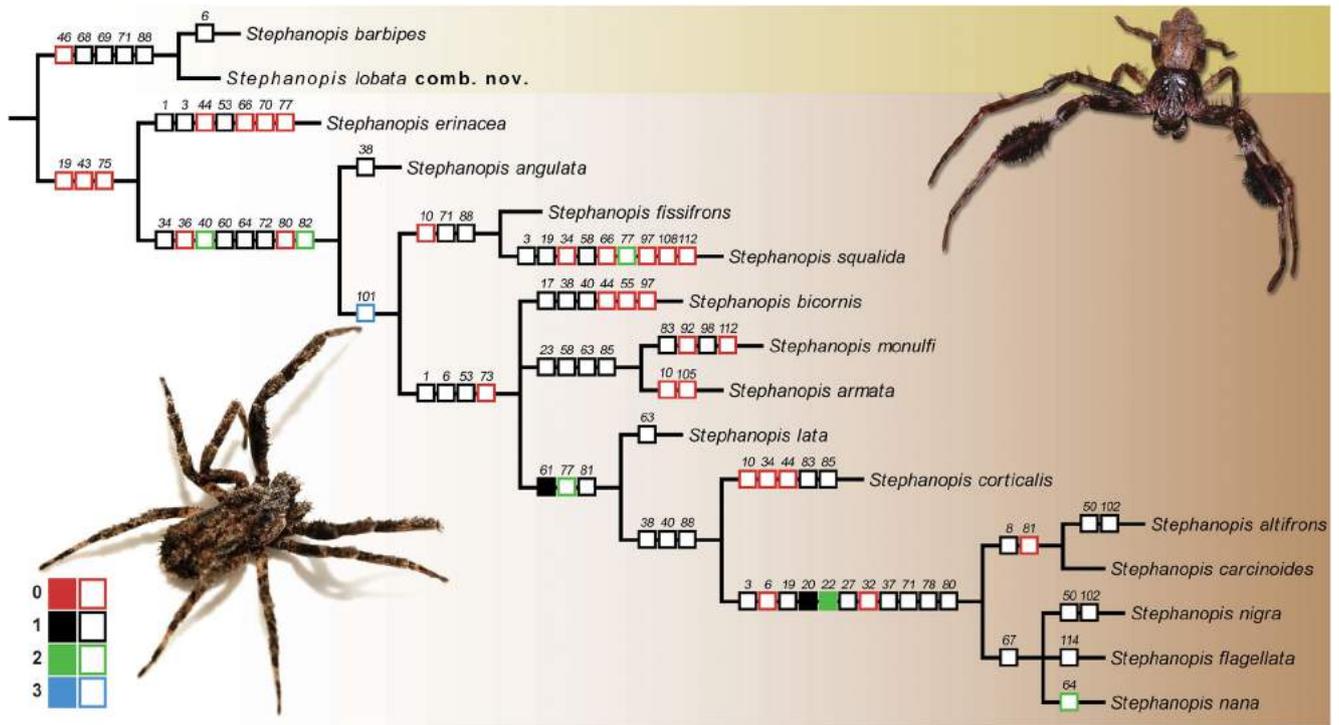
Fig. 4 Character transformations in *Stephanopis* (*stricto sensu*) based on the topology of the most congruent tree ($K = 17.89$). Filled squares represent synapomorphies and those in white are homoplastic characters. Character states: red (0); black (1); green (2); blue (3). 1—"*lata* group" and "*altifrons* group" (sensu Machado et al. 2019b)

Epicadus (in part), *Epicadinus*, the "*cambridgei* group" (sensu Machado et al. (2019b)) and for all Neotropical species of *Stephanopis* except *St. championi* + *Stephanopis* sp. 1. The square-ended/bifid abdomen, defined here by the presence of dorsolateral projections on the opisthosoma in the absence of both median and ventrolateral ones, was thought to be a diagnostic character for *Sidymella* (Machado et al. 2019a); however, this feature appeared in 11 other distinct clades.

Although highly diverse in regard to their somatic characteristics, it is accepted that the genital morphology in Thomisidae is quite conservative (Benjamin 2011). However, our findings point to a significant number of both
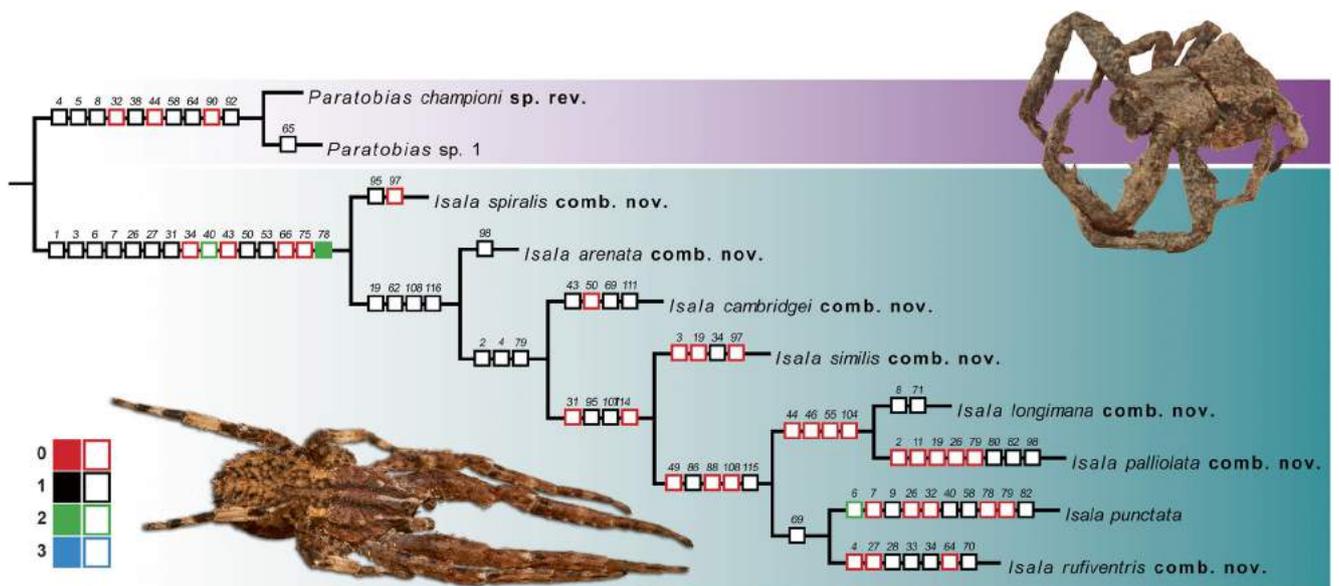
Fig. 5 Character transformations and detail of the dichotomy between the *Isala* and *Paratobias* **gen. rev.** based on the topology of the most congruent tree ($K = 17.89$). Filled squares represent synapomorphies and those in white are homoplastic characters. Character states: red (0); black (1); green (2); blue (3)
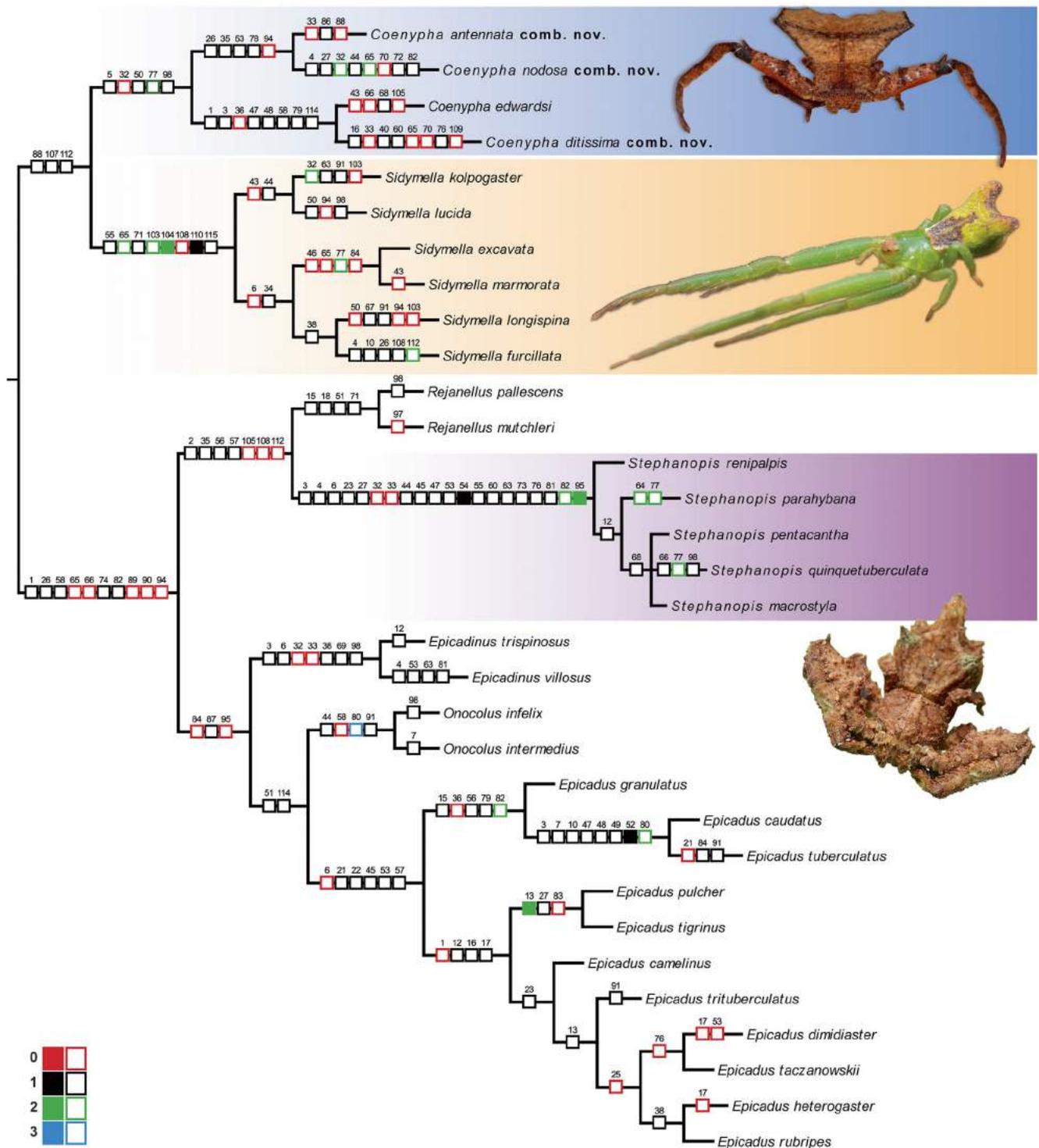
Fig. 6 Character transformations, detailed topology of the relationships between "*ditissima* clade" (blue) and *Sidymella* (stricto sensu); emergence of the "*pentacantha* clade" (purple) as part of the "*Epicadus* group" based on the topology of the most congruent tree (*K* = 17.89). Filled squares represent synapomorphies and those in white are homoplastic characters. Character states: red (0); black (1); green (2); blue (3)

sexual and somatic traits behaving as homoplasies along the tree (Figs. 5, 6, 7 and 8). The topology discussed here is for the most part concordant with what was noted by the authors

mentioned above. The relatively weak branch supports seem to be related to repeated state reversals and to a high number of homoplastic characters (Figs. 5, 6, 7 and 8). The increase in
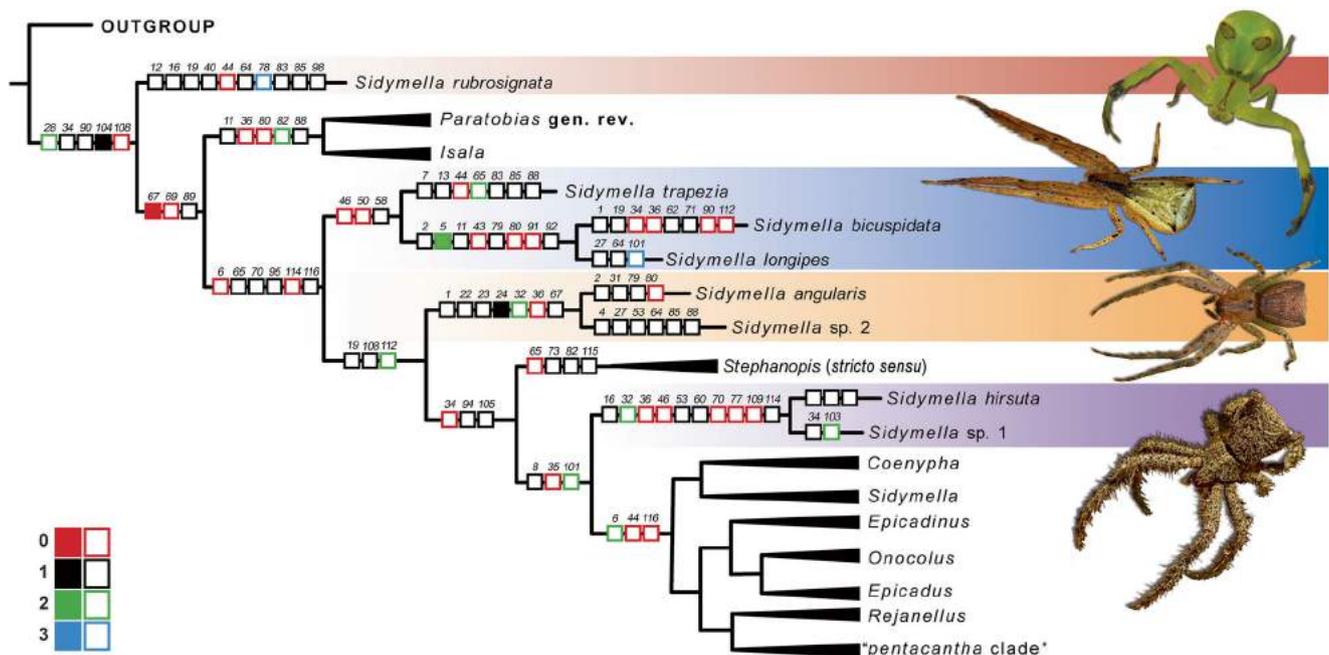
Fig. 7 Section of the working phylogenetic hypothesis detailing the character transformations and relationships between the "*angularis* clade" (orange), *Sidymella rubrosginata* (red), "*trapezia* clade" (blue) and "*hirsuta* clade" (purple). Filled squares represent synapomorphies and those in white are homoplastic characters. Character states: red (0); black (1); green (2); blue (3)

the data input, however, allowed a new interpretation regarding the composition of both *Stephanopis* and *Sidymella* as well as the relationships between these genera.

Stephanopis

"*altifrons* clade"

In the taxonomic work provided by Machado et al. (2019b), the authors suggested the possible existence of three distinct groups of species in the genus ("*cambridgei* group", "*altifrons* group" and "*lata* group"). This latter was not independently recovered by non-ambiguous synapomorphies as alpha-taxonomy insights previously suggested. Instead, all its component species emerged in a single and weakly supported clade with species assigned to the "*altifrons*" group" (sensu Machado et al. (2019b)). Moreover, a dichotomy between this major clade with *Stephanopis barbipes* Keyserling, 1890 + *St. lobata* **comb. nov.** was recovered based on three homoplastic features. Despite its considerable heterogeneity, hereinafter we call this group as the "*altifrons* clade".

Among the species that comprise *Stephanopis*, *Stephanopis erinacea* Karsch, 1878 stands out as the only insular taxon, occurring far from the Australian territory, being recorded in the Fiji Islands. The restricted distribution and specific selective pressures possibly suffered by this species may have contributed to the evolution of a highly apomorphic organism that, although retaining some important similarities with its congeners, had developed distinct somatic features

that are not observed in any other *Stephanopis* species. Besides that, the male of *St. erinacea* is unknown; thus, a significant portion of the matrix related to male genitalic features was not scored for this taxon, possibly contributing to the poor resolution and the instability of the clade. The unpredictable behaviour of this terminal taxon in the EW analyses led us to perform another method for topology test. As a result, the removal of this wild card through pruning in equal weights analysis resulted in gaining six additional nodes in the outgroup resolution while the topology of the "*altifrons* clade" remained stable (Appendix 3). One way or another, the group presented in the main hypothetical reconstruction was supported by homoplasies (Fig. 8): the absence of dorsolateral projections on the opisthosoma and absence of both macrosetae on the ocular quadrangle (char. 43, state 0; see Fig. 9g) and clypeus margin (char. 19, state 0; see Fig. 9g). All males of the "*lata* group" (sensu Machado et al. (2019b)) (e.g. *Stephanopis lata* O. Pickard-Cambridge, 1869, *Stephanopis armata* L. Koch, 1874, *Stephanopis monulfi* Chrysanthus, 1964, *Stephanopis bicornis* L. Koch, 1874, *Stephanopis angulata* Rainbow, 1899, *Stephanopis corticalis* L. Koch, 1876, *Stephanopis fissifrons* Rainbow, 1920 and *Stephanopis squalida* Machado, 2019) present a diagnostic structure on the dorsal portion of their cymbium: a group of arrow-shaped setae arranged close together that looks similar to a small brush (char. 117, state 1; see Fig. 20h). However, this structure was interpreted as ambiguous in our analyses because the male of *St. erinacea* is unknown, and palpal characters are missing for this terminal taxon. Thus, this feature

was not represented along the tree branches. According to Dr. Martín Ramírez (pers. comm), this setae cluster probably has a chemosensory function. High-magnification SEM images of these structures were not taken, so further investigations should be carried out to verify this assumption. Males of the "*lata* group" (sensu Machado et al. (2019b)) also have a truncated branch on the ventral portion of the RTA (char. 106, state 0; see Fig. 14a) while neither females nor males in this group have the remarkable cephalic prominence observed in the "*altifrons* group" (sensu Machado et al. (2019b)) (Fig. 11a). This latter emerged as a derivate group with its putative synapomorphies being the high cephalic portion (char. 22, state 2; see Fig. 10d) bearing a pair of lateral tubercles (char. 20, state 1; see Fig. 9g) (Fig. 5). Comparative studies with morphometric and ecological approaches must be encouraged to test if the flattened habitus of species of the "*altifrons* group" (sensu Machado et al. (2019b)) could be related to a specific niche specialization (hunting on trunks and under tree bark), as Dias and Brescovit (2003) suggested for *Pachistopelma rufonigrum* Pocock, 1901, a theraphosid spider that lives in bromeliads, or *Morebilus plagusius* Platnick, 2002, a dorsoventrally flattened trochanteriid adapted to live in crevices and under sun-exposed rocks (Goldsbrough et al. 2004). According to Goldsbrough et al. (2004), the development rate of *M. plagusius* specimens is increased due to the high temperatures of the surfaces where they live under.

Recovered by five homoplastic characters and presenting significant nodal stability and branch supports, the clade (*St. barbipes* + *Si. lobata*) is clearly the most controversial clade in *Stephanopis* (Figs. 1 and 3). A series of leg characteristics set these two species apart from the rest of the main clade. Their distinct trichobothria disposition (char. 46, state 0; see Fig. 12f), morphology of tarsal claws (char. 69, state 1; see Fig. 13e) and density of the setae tuft, as well as the length proportion between their metatarsal macrosetae (char. 71, state 1; see Fig. 14a), might explain the divergence from other species of the genus. However, genitalic features such as the presence of pars pendulum on male palp (char. 115, state 1; see Fig. 20a, g) and membranous chamber-like copulatory ducts in female genitalia (char. 88, state 1; see Machado et al. (2019b), Fig. 37d) pull them together as the sister clade of the "*lata* + *altifrons*" group. The recovery of *Si. lobata* as a sister species to *St. barbipes* was strongly supported, and for that reason as well as the presence of diagnostic genitalic characters, the most parsimonious decision was to keep this latter species in *Stephanopis* and propose the transference of *Si. lobata* as it clearly does not fit in *Sidymella* instead of erecting a new genus to accommodate both. However, there are substantial somatic differences with other *Stephanopis* species and we highlight that the placement of *St. barbipes* and *St. lobata* **comb. nov.** (formally proposed hereinafter) is highly questionable and deserves future investigation.

"*cambridgei* clade"

Species previously assigned to the "*cambridgei* group" by Machado et al. (2019b) were recovered as a stable clade with *I. punctata* nested within (Fig. 5). The similarities with *Isala* include the longitudinal dual band on the prosoma (char. 13, state 1; see Fig. 15h), the flattened cephalic area, five ventral macrosetae on tibiae I and II (char. 13, state 1; see Fig. 15h) in females, and the presence of modified setae on these same leg segments for males (char. 62, state 1; see Fig. 13c). This latter character was mentioned by Machado et al. (2019b), who described it as a set of long, thin and filiform barbs. All parsimony analysis using implied weighting schemes recovered this clade (Fig. 2) with relatively high support (Fig. 3), with its component species presenting the granular surfaced opisthosoma (char. 78, state 2; see Fig. 13f) as the only unambiguous synapomorphy. This group was also recovered by the presence of barbed clavate setae on their opisthosoma (Fig. 16b), which according to Gawryszewski (2014) are positively related to the effectiveness of becoming camouflaged through debris retention. This author found three different types of setae in *St. altifrons* and *St. cambridgei* that seem to be specialized for retaining organic particles. While *St. altifrons* present all three types of elongated and branched setae (generalized here as "needle-shaped"), *St. cambridgei* have just one, which we coded as "clavate", while Gawryszewski (2014) describes it as cuneiform, barbed and dorsally striated. We agree with Gawryszewski (2014) that this variation in setae morphology could be related to selection for retaining different types of debris, which might indicate niche partitioning. The paraphyletic relationship between these clades can also be observed through differences in sexual traits. While males of *St. altifrons* have a RTAvbr and females present a shallow epigynal plate with exposed copulatory openings (char. 91, state 0; see Machado et al. (2019b), Fig. 3c and e), the "*cambridgei* group" gathers males without RTAvbr and females with well-developed folds delimiting the atrium and covering the copulatory openings (see Machado et al. 2019b, Fig. 18c). Therefore, the morphological distinctions listed above are seen as evidence indicating that the entire "*cambridgei* clade" belongs to a genus other than *Stephanopis*. As the taxonomy of the entire clade was recently revised by Machado et al. (2019b), we suggest here the transference of all species of the "*cambridgei* group" to *Isala*.

Benjamin (2011) recovered *St. cambridgei* nested in *Sidymella*, having a close relationship with *Si. lucida*, the type species of this genus. In our results, on the other hand, *St. cambridgei* and other Australian species belonging to the "*cambridgei* clade" have emerged as sister of a small clade of *Stephanopis* species with distribution restricted to Central America (Fig. 5). This dichotomy, though, was weakly supported as it was recovered by only five weighting schemes in our sensitivity analysis; thus, it is probably spurious (Fig. 2).

Three of the five homoplasies that recover the dichotomy between these clades are based on setae morphology and its microstructures (Fig. 5); however, their component species are noticeably distinct with regard to their copulatory structures (such as the absence of RTA for *Stephanopis* sp. 1) and most of its somatic characters. Moreover, under 10 implied weighting schemes, the *St. championi* + *Stephanopis* sp. 1 clade emerged independently or somehow unrelated to the "*cambridgei* clade" (Fig. 2).

"*championi* clade"

Simon (1903) synonymized *Paratobias* F. O. Pickard-Cambridge, 1900 with *Stephanopis* arguing that the disposition and curvature of the eye rows were highly variable among the species of this group. Not only was this decision misleading, as this author did not present any major comparison among these genera, there are other somatic characters that never seem to have been considered, such as the different number of tibial macrosetae (Char. 64), femoral tubercles (Char. 50), presence or absence of the thoracic median spire (Char. 23) and the shape of the opisthosoma (Chars. 74, 75 and 76). The paraphyletic relationship with other species of *Stephanopis*, low branch support values and weak nodal stability are indicative that "*championi* clade" should be considered as a distinct genus. Not only somatic but also genitalic features of *St. championi* such as the absence of RTA on male palp did not match those observed in the "*cambridgei* clade" or the "*altifrons* clade". Thus, in order to assume the most parsimonious taxonomic decision, we propose that the *St. championi* should be restored to its original genus, *Paratobias* (see the "Taxonomy" section).

"*pentacantha* clade"

While two species of *Stephanopis* from Central America emerged close to the "*cambridgei* clade", the remaining Neotropical species were placed inside the "*Epicadus* group" (Fig. 6), a potential clade suggested by Silva-Moreira and Machado (2016) and partially recovered by Machado et al. (2017). A similar topology was recovered by Wheeler et al. (2017) with considerable support. Machado et al. (2017) recovered *St. altifrons* as closely related to the Neotropical species; however, the less inclusive approach on Australian representatives of the genus prevented these authors from considering genitalic features that have come to be crucial for elucidating the relationships in *Stephanopis*. In addition to the presence of a median spire on the thoracic portion of the prosoma (Char. 23, state 1; see Fig. 15f) and the opisthosoma bearing five conical projections, this clade also diverges from *Stephanopis* by a series of sexual traits: male palp with a dorsally curved (Char. 101, state 2) and single-tipped RTA, absence of tegular ridge and tegulum smooth surface (Char.

108, state 0; Char. 110, state 0; see Fig. 17b). Differing from *St. altifrons* and its correlated terminal taxa, this clade is composed of species where males lack the PrsP (Char. 115, state 0) and the CP (Char. 116, state 0). The female genitalia has a single pair of elliptical and smooth spermathecae, whereas females of *Stephanopis* have coiled spermathecae (Char. 89) with glandular heads (Char. 90) that are preceded by chamber-like copulatory ducts (Char. 86).

Along with *Rejanellus*, these are now the only known representatives in the "*Epicadus* group" (sensu Silva-Moreira and Machado (2016)) with females having short CD and males lacking the RTAvbr on their palpi. Although sharing these features, the "*pentacantha* clade" presents other characteristics (e.g. five conical projections on the opisthosoma; leaf-shaped setae; presence of MS) that set them apart from its sister genus. Its component species were grouped with strong branch support (Fig. 3) and recovered by two synapomorphic characters: presence of ventral macrosetae on patellae I and II (Char. 54, state 1; see Fig. 13b) and male palp bearing pear-shaped tegulum (Char. 95, state 2; see Fig. 17b). Despite the dichotomy with *Rejanellus*, the evidences listed above are interpreted as sufficient to justify the proposition of the "*pentacantha* clade" as a new genus. Although well supported, the internal topology of the group is poorly resolved. This is due to the conservative morphology of its component species, which can only be distinguished from each other by details of their genitalia, such as the curvature, size and shape of the RTA and embolus, or the presence/absence of the median septum on the epignyal plate. A study focusing on their taxonomy is essential to explore these morphological aspects, as well as updating descriptions and diagnostic structures.

"*ditissima* clade"

The relationship between *Stephanopis* species from the Andean region and *Coenypha* was well supported by molecular evidence (Wheeler et al. 2017) and corroborated by morphologic studies (Machado et al. 2017). Although preliminary, the insights and results obtained by Machado et al. (2017) regarding the topology of the clade remained consistent in comparison to what we found in the present work (Fig. 2). According to Machado et al. (2017), the coincident geographical distribution and several similarities regarding the morphology of copulatory structures of these species could indicate possible synonymies or new combinations between the two genera. The inclusion of two more species of *Stephanopis* from the Andean region in our data matrix aimed to test if those previous hypotheses could be corroborated through broader morphological comparisons. The disposition and shape of copulatory structures in *Coenypha*, such as the wide median septum, exposed copulatory ducts, acute RTA, laminar embolus and abdominal projections laterally disposed, are remarkably similar to what are observed in *S. ditissima*, *Stephanopis nodosa* (Nicolet, 1849) and *St. antennata* Tullgren, 1902. The node

gathering these "Andean *Stephanopis*" in a clade with *Coenypha* is shown to be stable, being recovered under all weighting schemes and Bayesian analysis (Fig. 2), and here called "*ditissima* clade". The group with four species presented significant branch supports (Fig. 3), being recovered by five homoplastic characters (Fig. 6) and corroborating previous evidences based on morphological (Machado et al. 2017) and molecular data (Wheeler et al. 2017). Therefore, consider that the *Stephanopis* species belonging to the "*ditissima* clade" should be transferred to *Coenypha* (Fig. 6).

The close relationship between *Coenypha* and the "Neotropical *Sidymella*" was similarly obtained in Wheeler et al. (2017). Additionally, our findings show these two sister clades being related to the entire "*Epicadus* group". The *Coenypha* + "*Neotropical Sidymella*" relationship was recovered not only by the presence of membranous and hyaline copulatory ducts of the female genitalia (Char. 88, state 1) but also by males bearing a flattened and laminar embolus (Char. 107, state 1; see Fig. 8(3)f) resting on tegulum (Char. 112, state 1).

Sidymella

According to the diagnosis provided by Machado et al. (2019a), *Sidymella* and *Coenypha* have a series of similar characteristics related to the epigynum and the male palp. This view is correct if only the Neotropical species of *Sidymella* are being considered in such a comparison. The Australian representatives of the genus, although presenting some features common to the Neotropical species, such as the presence of spiniform macrosetae on the mesial surface of femora I (interpreted here as dorsolateral setiferous tubercles) (Char. 49, state 1; see Fig. 14a and b) and epigynum with accessory glandular heads (Char. 90, state 1; see Fig. 8(0)g), emerged in four different clades (Fig. 2). The evidence obtained through our data also suggest that the bifid opisthosoma, a character that was still being recently considered by Machado et al. (2019a) as valid way to recognize and distinguish *Sidymella* from other stephanopines, in fact appeared in 11 different groups. Thus, contrary to what previous taxonomic works have shown (Lise 1973; Machado et al. 2019a), the presence of dorsolateral humps on the abdomen of these spiders seems to be insufficient to undoubtedly characterize the genus. Moreover, the composition of *Sidymella* as a natural group is implausible if we consider that this and other somatic characters shared between Neotropical and Australian species of *Sidymella* as the result of a possible adaptive convergence to support the same hunting behaviour. These spiders are commonly found on tree branches and plant stems with their forelegs close together and directed frontwards, camouflaging themselves as twigs (pers. obs.). The polyphyletic emergence of *Sidymella*, as currently circumscribed, is corroborated by molecular evidence presented by Wheeler et al. (2017).

Similar to our results, the findings presented by these authors recover the Neotropical species of *Sidymella* as sister group to *Coenypha* (Fig. 6) while Australian species are related to *Stephanopis* (here, represented by the emergence of *St. barbipes* + *St. lobata* **comb. nov.**) (Fig. 7). Although visibly distinct regarding their somatic features, the palpal architecture of *Sidymella* species from the Australian region is similar to those of *Stephanopis* by presenting CP (Char. 116, state 1; see Fig. 18h), filiform embolus (Char. 107, state 0; see Fig. 18h) and the RTA acute (Char. 103, state 1; see Fig. 18h) with grooved surface (Char. 104, state 1).

The group composed by *Si. lucida* and five other species of *Sidymella* recorded in the Neotropical region (World Spider Catalog 2020) was recovered with good stability (Fig. 2). The clade also presented significant branch supports (Fig. 3), being sustained by two synapomorphies that set them apart from Australian species: RTA with nodose texture (Char. 104, state 2; see Fig. 19b) and tegulum with scaled surface (Char. 110, state 1; see Fig. 20d). Thereby, although we call this group the "*lucida* clade" throughout the discussion, we anticipate that this is the only clade that should truly be considered as *Sidymella* (stricto sensu). Australian species currently attributed to this genus are hereinafter treated as "dissident" clades, which should be proposed as new genera in future taxonomic works (Fig. 7).

"angularis clade"

The maximum likelihood analyses performed by Sirvid et al. (2013) for 28S and H3 sequences and combining COI, 28S, H3 and ND1 data are consistent with the morphological evidence presented here in showing some degree of relationship between *Si. trapezia* + *Si. longipes* and *S. angularis* (Fig. 2). Likewise, we obtained good support values for the clade that gathers species from New Zealand (*Si. angularis* + *Sidymella* sp. 2). This clade seems to be more related to *Stephanopis* than to its congeneric species from Australia (e.g. *Si. trapezia* + *Si. longipes*). Despite somatic similarities have been observed and scored for both the "*longipes* clade" and the "*angularis* clade", features common to this latter and *Stephanopis* (stricto sensu), especially regarding the architecture of copulatory structures, seem to outweigh the body features (even the diagnostic shape of the opisthosoma) that taxonomically would place them in *Sidymella*. This is the main reason why we also justify the transference *St. lobata* **comb. nov.**, besides aiming for the most stable and parsimonious taxonomic decision. More importantly, we see this as another indicative that the bifid/trapezoidal opisthosoma in *Sidymella* as currently accepted can be a evolutive convergence that reflects the hunting/cryptic behaviour of distinct groups that are not necessarily closely related in taxonomic and phylogenetic terms. According to Sirvid et al. (2013), the recent establishment of *Si. longipes* and *Si. trapezia* in New Zealand suggests a capacity of long-range dispersal over water, contrary to the

vicariant hypotheses usually considered to explain the distribution of stephanopines in the Australian region. Although Sirvid et al. (2013) had found molecular evidence supporting separate New Zealand lineages within the Australasian stephanopines, the hypothetical reconstruction discussed here suggests a proximity between *Si. angularis*, a common species that is widely spread in New Zealand, and *Sidymella* sp. 2, recorded along the east coast of Australia (Fig. 3). The node grouping the two species was recovered by all optimality criteria except equal weights (Fig. 2) and showed significant branch supports (Fig. 3). The clade presented one synapomorphy: the presence of dual median spire on the thoracic portion of the prosoma (Char. 24, state 1; see Fig. 15h), a feature that was mentioned by Bryant (1933) and Sirvid et al. (2013) as a putative character to suggest a new generic assignment to *Si. angularis*. There is a significant number of undescribed species in Australian collections that present similar characteristics observed in *Si. angularis* and *Sidymella* sp. 2 (pers. obs.). An analysis with a broader sampling, molecular data and a biogeographical approach would help to elucidate the phylogenetic relationships and dispersal mechanisms used by these crab spiders along the Australian region.

"hirsuta clade"

The "*hirsuta* clade" is formed by spiders that resemble *Epicadinus* by their "spiny" habitus, with long and needle-shaped setae covering their entire prosoma (Char. 11, state 0 and 2), opisthosoma (Char. 80, state 1; see Fig. 21h) and legs. The group was supported by 10 homoplastic characters and one synapomorphy: RTAvbr spoon-shaped (Char. 106, state 3; see Fig. 19e). Because of how the characters were treated in our analyses, this ambiguous feature was not shown along the branch on the working phylogenetic hypothesis. Nevertheless, the emergence of the genus by itself is held by strong branch supports (Fig. 3) and good nodal stability (Fig. 2). As observed in *Stephanopis*, the male palp architecture of species of the "*hirsuta* clade" is characterized by the presence of a RTAvbr, well-developed CP, oval-shaped tegulum and filiform embolus meandering at its distal portion (whip-like). The arrangement and shape of copulatory structures of females, although slightly different from those of *Stephanopis*, also show some degree of resemblance. Females of the "*hirsuta* clade" have flattened, narrowed and tubular copulatory ducts (Char. 86, state 0; Fig. 16e, g) and spermathecae significantly longer than those of *Stephanopis*. Despite having an opisthosoma with a pair of "protruding corners" (dorsolateral projections), a feature considered by Koch (1874) to justify the original description of *Si. hirsuta* in *Sidymella*, other somatic characters (e.g. number and arrangement of tibial and metatarsal macrosetae; disposition of teeth of the tarsal claws) wildly differ from those of the species type of this genus. The relationship of the "*hirsuta* clade" with the clade composed of the "*Epicadus* group" and (*Coenypha* + *Sidymella*) was based on three highly homoplastic characters, each presenting numerous state reversals. Moreover, both Bremer indexes and symmetric resampling analyses presented low support values for this more inclusive clade (Fig. 3) as well as sensitivity analyses showing weak nodal stability in this section of the topology (Fig. 2). Such results, along with the unpredictable behaviour of the clade, suggest that the placement of the "*hirsuta* clade" is particularly arguable. Similarities and shared characters between this group and *Stephanopis*, in addition to their coincident geographical distribution, must also be considered as evidence that the placement of the "*hirsuta* clade" with most Neotropical stephanopine genera sampled in this study is questionable and most likely to be spurious.

"trapezia clade"

The relationship between *Si. trapezia* and the species that Sirvid et al. (2013) call "near *corticalis*" showed to be poorly supported by maximum likelihood analyses of COI sequence data. The uncertainty regarding the species identity and low sampling of Australian taxa in that study were possibly the main reasons of such result. Here, morphological traits did not recover *Si. trapezia* as close related to *St. corticalis*, let alone the placement of *Si. longipes* in *Stephanopis*. Both these *Sidymella* species were grouped in the same clade with *Si. bicuspidata* by three homoplasies related to leg characteristics (Fig. 7). However, the topology of the group was inconsistent and weakly supported, sometimes with *S. trapezia* behaving as a wildcard and occasionally *Si. bicuspidata* + *Si. longipes* emerging separately. Every so often, parsimony with implied weights recovered only *S. trapezia* as a sister group to the "*cambridgei* clade" and occasionally in a clade with *Si. bicuspidata* + *Si. longipes* as a sister to the "*cambridgei* clade", being this latter in a dichotomy with *Stephanopis*. As observed for the "*angularis* clade" and "*hirsuta* clade", the "*trapezia* clade" also shares with the "*altifrons* clade" and the "*cambridgei* clade" the presence of CP close to the RTA of the male palp. Such structure seems to be constant in these groups of Australian stephanopines and might contribute to their weakly resolved relationship in the face of their remarkable somatic disparities.

The "*trapezia* clade" is formed by taxa that clearly do not fit with the recently updated diagnosis of *Sidymella* and the taxonomic background presented by Machado et al. (2019a) was corroborated by the emergence of the Neotropical species far apart from those hitherto called "Australian *Sidymella*". Additionally, the analyses of molecular data presented by Sirvid et al. (2013) show *Si. trapezia* emerging independently from other taxa or, when grouped in a more inclusive clade, presenting low values of branch support. Therefore, we believe that although significantly heterogeneous and lacking good nodal stability, the "*trapezia* clade" must be proposed

as a new genus in a future taxonomic work. Only then, the most parsimonious decision will be taken, avoiding the maintenance of a paraphyletic status for *Sidymella*, erection of a monospecific genus to accommodate only *Si. trapezia* or the proposition of the three species as *incertae sedis*.

The species *Si. rubrosignata* behaved unpredictably, presenting even weaker support and being more unstable than the "*trapezia* clade". Alternative resolutions represented this species emerging within the "*Epicadus* group" due to the presence of characters such as the disk-shaped tegulum on the male palp (Char. 95, state 0) and the median longitudinal band (Char. 12, state 1) with a guanine white spot on the thoracic portion (Char. 16, state 1), or independently (as shown in the discussed tree), but always as sister to the remaining taxa of the ingroup (Fig. 2). Considering all analyses and morphological evidence presented here, once again, justifying the description of a stephanopine species in *Sidymella* based merely on the presence of a pair of lateral projections on the opisthosoma has proven to be insufficiently grounded and inaccurate. None of the diagnostic features regarding the male palp architecture or copulatory duct disposal of species of *Sidymella* is observed in *Si. rubrosignata*. The independent emergence of this taxon is recovered by 10 homoplastic characters and supports Simon's (1895) insights considering it as a group apart from *Stephanopis* as well (Fig. 7). Thus, we believe that *Si. rubrosignata* deserves a new generic assignment.

Conclusions

The hypothetical reconstruction presented in this study is based on the most comprehensive morphological data matrix focusing on Stephanopinae to date. Our results corroborate classic taxonomic insights recovering the four groups mentioned by Simon (1895) as doubtful, as distinct clades. Recent phylogenetic analyses based on morphological (Benjamin 2011; Ramírez 2014) and molecular (Benjamin et al. 2008; Wheeler et al. 2017) data were shown to be congruent with the present findings, suggesting that both *Stephanopis* and *Sidymella* are polyphyletic, as currently circumscribed. Different approaches and methodologies were applied to estimate nodal stability and branch supports, seeking to base desired taxonomic changes with plausibility and consistency.

Despite certain morphological heterogeneity between its representatives and low branch support, *Stephanopis* (stricto sensu) is recognized here as a group formed only by species of the "*altifrons* clade", gathering all Australasian representatives that Machado et al. (2019b) attributed to the "*lata* group" and "*altifrons* group", in their taxonomic revision. The genus also includes the clade *St. barbipes* + *St. lobata* **comb. nov.** in dichotomy with all its remaining congeneric species. On the

other hand, *Sidymella* (stricto sensu) should be treated as a genus comprised solely by species of the "*lucida* clade".

The outgroup relationships are partially concordant with those obtained by Benjamin (2011), Ramírez (2014) and Machado et al. (2017). Divergences were expected once we focused on sampling the ingroup extensively, while the high diversity of the outgroup genera remained poorly represented. These specimens were scored to polarize the characters, so their weakly supported relationships, as shown in the hypothetical reconstruction, are preliminary and insufficiently accurate to bring forth grounded discussions. The lack of resolution as well as the weak support obtained by resampling analysis and relative Bremer indexes for deep branches is a result of a highly homoplastic matrix with many missing data and state reversals. Notwithstanding, the significant amount of either homoplastic or synapomorphic characters showed that terminal clades are in general recovered with good nodal stability regardless of how the data are analysed. This constancy obtained with a phylogenetic approach, along with extensive studies on the morphology of the group, provided a more thorough understanding of its relationships, compiling evidence to ensure stable taxonomic decisions in the future.

Taxonomy

Thomisidae Sundevall, 1833
Stephanopinae O. Pickard-Cambridge, 1871
***Stephanopis* O. Pickard-Cambridge, 1869**
Type species: *Stephanopis altifrons* O. Pickard-Cambridge, 1869

Diagnosis. The genus *Stephanopis* (stricto sensu) is composed of bark-dwelling spiders with a dorsoventrally compressed, flattened habitus. They have high cephalic prominence, well-developed clypeus and opisthosoma rounded at the rear or ending abruptly (pentagonal in dorsal view). The genus can also be distinguished by males having palpi with retrolateral CP, pars pendulum, embolus rigid at its proximal portion, becoming gradually flexible, filiform and meandering post-apically; the RTA is wide, obtuse and single-tipped in all species of the "*lata* group" (sensu Machado et al. (2019b)). However, males of derivate species belonging to the "*altifrons* group" (sensu Machado et al. (2019b)) (and *St. barbipes*) present acute and bifid RTA (well-developed RTAvbr). Female genitalia is characterized by the epigynal plate with shallow, flattened atrium, slit-shaped CO and wide, chamber-like copulatory ducts preceding a pair of asymmetric cylindrical spermathecae.

Taxonomic acts
Sidymella lobata (L. Koch, 1874): Syntype female from Sydney, Australia (ZMB 3414, examined). Transferred to

Stephanopis—*Stephanopis lobata* (L. Koch, 1874) **comb. nov.**

Composition. The genus *Stephanopis* (stricto sensu) is composed of 16 valid species distributed across Australia and Southeast Asia: *Stephanopis altifrons* O. Pickard-Cambridge, 1869; *Stephanopis angulata* Rainbow, 1899; *Stephanopis armata* L. Koch, 1874; *Stephanopis barbipes* Keyserling, 1980; *Stephanopis bicornis* L. Koch, 1874; *Stephanopis carcinoides* Machado, 2019; *Stephanopis corticalis* L. Koch, 1876; *Stephanopis erinacea* Karsch, 1878; *Stephanopis fissifrons* Rainbow, 1920; *Stephanopis flagellata* Machado, 2019; *Stephanopis lata* O. Pickard-Cambridge, 1869; *Stephanopis lobata* (L. Koch, 1874) **comb. nov.**; *Stephanopis monulfi* Chrysanthus, 1964; *Stephanopis nana* Machado, 2019; *Stephanopis nigra* O. Pickard-Cambridge, 1869 and *Stephanopis squalida* Machado, 2019.

Note. Other valid species that are currently described in *Stephanopis* that were not listed above will be properly addressed in future taxonomic works where new genera will be officially proposed.

Sidymella Strand, 1942
Type species: *Sidymella lucida* (Keyserling, 1880)

Diagnosis. The component species of *Sidymella* (stricto sensu) can be distinguished from other thomisids by the presence of stout spines on the mesial surface of femur I and macrosetae above their ALE. Males are diagnosed by their long and laminar embolus with well-developed pars pendulum curving at their terminal portion. Unlike other stephanopines, which have smooth-surfaced RTAs or with parallel creases on it, males of *Sidymella* present a rounded RTA with nodose texture and truncated short RTAvbr; a prominent trichobotrium can be observed on the dorsum of the palpal tibia. Females differ from those of other genera by their coiled copulatory ducts leading to a pair of walnut-shaped spermathecae internally compartmentalized in small chambers.

Composition. The genus *Sidymella* (stricto sensu) is composed of six valid species with distribution range restricted to the Neotropical region: *Sidymella lucida* (Keyserling, 1880); *Sidymella excavata* Machado & Guzati, 2019; *Sidymella furcillata* (Keyserling, 1880); *Sidymella longispina* (Mello-Leitão, 1943); *Sidymella marmorata* Machado & Guzati, 2019 and *Sidymella kolpogaster* (Lise, 1973).

Note. Other valid species that are currently described in *Sidymella* that were not listed above will be properly addressed in future taxonomic works where new genera will be officially proposed.

Coenypha Simon, 1895
Type species: *Coenypha edwardsi* (Nicolet, 1849)

Diagnosis. Species of *Coenypha* are similar to those of *Sidymella* due to the presence of a retrolateral trichobothria on the male palpal tibia and the disposition of the coiled and membranous copulatory ducts of the female genitalia. However, species of *Coenypha* can be easily recognized by their flattened habitus, wide opisthosoma, enlarged femora I and slightly curved anterior tibiae. The epigynal plate of females has exposed openings separated by a robust median septum, and their copulatory ducts are wider than those of *Sidymella*, leading to a pair of walnut-shaped spermathecae (with several constrictions and internal subdivisions). The male palp bears a long and laminar embolus, as in *Sidymella*; however, in *Coenypha*, the tegulum is smooth and the RTA has grooves instead of nodes.

Taxonomic acts

Stephanopis antennata Tullgren, 1902: Holotype female from Aysén, Chile (NHRS, examined through photographs). Transferred to *Coenypha*—*Coenypha antennata* (Tullgren, 1902) **comb. nov.**

Stephanopis ditissima (Nicolet, 1849): Holotype female from Chile (MNHN 4176, examined). Transferred to *Coenypha*—*Coenypha ditissima* (Nicolet, 1849) **comb. nov.**

Stephanopis nodosa (Nicolet, 1849): Holotype female from Valdivida, Chile (MNHN 4194, examined). Transferred to *Coenypha*—*Coenypha nodosa* (Nicolet, 1849) **comb. nov.**

Composition. The genus *Coenypha* (stricto sensu) is composed, after the taxonomic acts proposed here, of seven valid species recorded for the Andean and Patagonian regions: *Coenypha edwardsi* (Nicolet, 1849); *Coenypha antennata* (Tullgren, 1902) **comb. nov.**; *Coenypha ditissima* (Nicolet, 1849) **comb. nov.**; *Coenypha fasciata* Mello-Leitão, 1926; *Coenypha fuliginosa* (Nicolet, 1849); *Coenypha lucasi* (Nicolet, 1849) and *Coenypha nodosa* (Nicolet, 1849) **comb. nov.**

Isala L. Koch, 1876
Type species: *Isala punctata* L. Koch, 1876

Diagnosis. Species of *Isala* resembles those of *Borboropactus* by their cryptic behaviour, with individuals frequently presenting lichen, sand and other soil particles attached to their tegument, and by the elongated body shape: prosoma and opisthosoma longer than wide, and anterior legs (I and II) aligning parallel to each other and directing frontwards. However, males of *Isala* can be recognized and distinguished by their well-developed palpi with cymbial projection, long and curved RTA and filiform embolus, lacking the median apophysis and the conductor, observed for *Borboropactus*. Females of this latter have acute lateral projections on the epigynal plate, known as "epigynal teeth", while females of *Isala* present a flattened atrium and folds of the epigynal plate strongly sclerotized, forming almost like "pockets" that protect and hide the copulatory ducts (in ventral view). Moreover, the ocular arrangement in *Isala* is characterized by the ALE noticeably bigger than the AME and the anterior eye row strongly recurved, while in *Borboropactus*

the anterior eyes are all similar in size and arranged in a straight row.

Taxonomic acts

Stephanopis arenata Machado, 2019: Holotype female from Scotia Sanctuary, New South Wales, Australia, 33° 07′ 36″ S 141° 10′ 40″ E (AMS KS.128001, examined). Transferred to *Isala*—*Isala arenata* (Machado, 2019) **comb. nov.**

Stephanopis cambridgei Thorell, 1870: Holotype female from Australia (NHRS 1163, examined). Transferred to *Isala*—*Isala cambridgei* (Thorell, 1870) **comb. nov.**

Stephanopis longimana Thorell, 1881: Holotype female from Cape York, Queensland, Australia, 10° 42′ S 142° 31′ E (MCSNG, examined). Transferred to *Isala*—*Isala longimana* (Thorell, 1881) **comb. nov.**

Stephanopis palliolata Simon, 1908: Syntype male from Wooroloo, Western Australia, Australia (ZMB 20726, examined). Transferred to *Isala*—*Isala palliolata* (Simon, 1908) **comb. nov.**

Stephanopis rufiventris Bradley, 1871: Holotype female from, Tia (40 km east of Walcha), New South Wales, Australia, 31° 12′ S 151° 48′ E (OUMNH 618, examined). Transferred to *Isala*—*Isala rufiventris* (Bradley, 1871) **comb. nov.**

Stephanopis similis Machado, 2019: Holotype female from Kanangra Boyd National Park (Boyd plateau near to Jenolan Caves), New South Wales, Australia, 34° 03′ S 150° 05′ E (AMS KS.30026, examined). Transferred to *Isala*—*Isala similis* (Machado, 2019) **comb. nov.**

Stephanopis spiralis Machado, 2019: Holotype female from Koorawatha National Reserve, New South Wales, Australia, 34° 01′ 55″ S 148° 35′ 59″ E (AMS KS.114827, examined). Transferred to *Isala*—*Isala spiralis* (Machado, 2019) **comb. nov.**

Composition. After the taxonomic acts listed hereinafter, we recognize *Isala* as a genus with Australian distribution, composed of eight valid species: *Isala punctata* L. Koch, 1876; *Isala arenata* (Machado, 2019) **comb. nov.**; *Isala cambridgei* (Thorell, 1870) **comb. nov.**; *Isala longimana* (Thorell, 1881) **comb. nov.**; *Isala palliolata* (Simon, 1908) **comb. nov.**; *Isala rufiventris* (Bradley, 1871) **comb. nov.**; *Isala similis* (Machado, 2019) **comb. nov.** and *Isala spiralis* (Machado, 2019) **comb. nov.**

Paratobias (F. O. Pickard-Cambridge, 1900) gen. rev.

Type species: ***Paratobias championi* (F. O. Pickard-Cambridge, 1900) sp. rev.**

Diagnosis. The genus *Paratobias* resembles *Coenypha* by the cryptic bark-dwelling habitus with dorsoventrally depressed prosoma. However, *Paratobias* can be distinguished by the presence of acute ocular projections, trapezoid opisthosoma and reduced AME (1/3 the size of the ALE). The female genitalia is characterized by a shallow and wide median field with copulatory openings positioned laterally, covered by the limits of the epigynal plate folds (Fig. 18c).

Composition. The genus *Paratobias* is currently represented by a single species: *Paratobias championi* (F. O. Pickard-Cambridge, 1900) **sp. rev.**

Data availability All data generated or analysed during this study are included in this published article (and its supplementary information files).

Compliance with ethical standards

Conflict of interest The authors declare that they have no conflict of interest.

Appendix

Fig. 8 Characters relative to dorsal habitus and prosoma of specimens sampled in the present analysis: **a** *Stephanopis lata*, frontal view. **b** *Sidymella excavata*, frontal view. **c** *Stephanopis pentacanha*, carapace. **d** *Epicadinus trispinosus*, carapace. **e** *Tmarus polyandrus*, carapace. **f** *Isala arenata* **comb. nov.**, dorsal habitus. **g** *Epicadus granulatus*, sternum. **h** *Borboropactus nyerere*, sternum
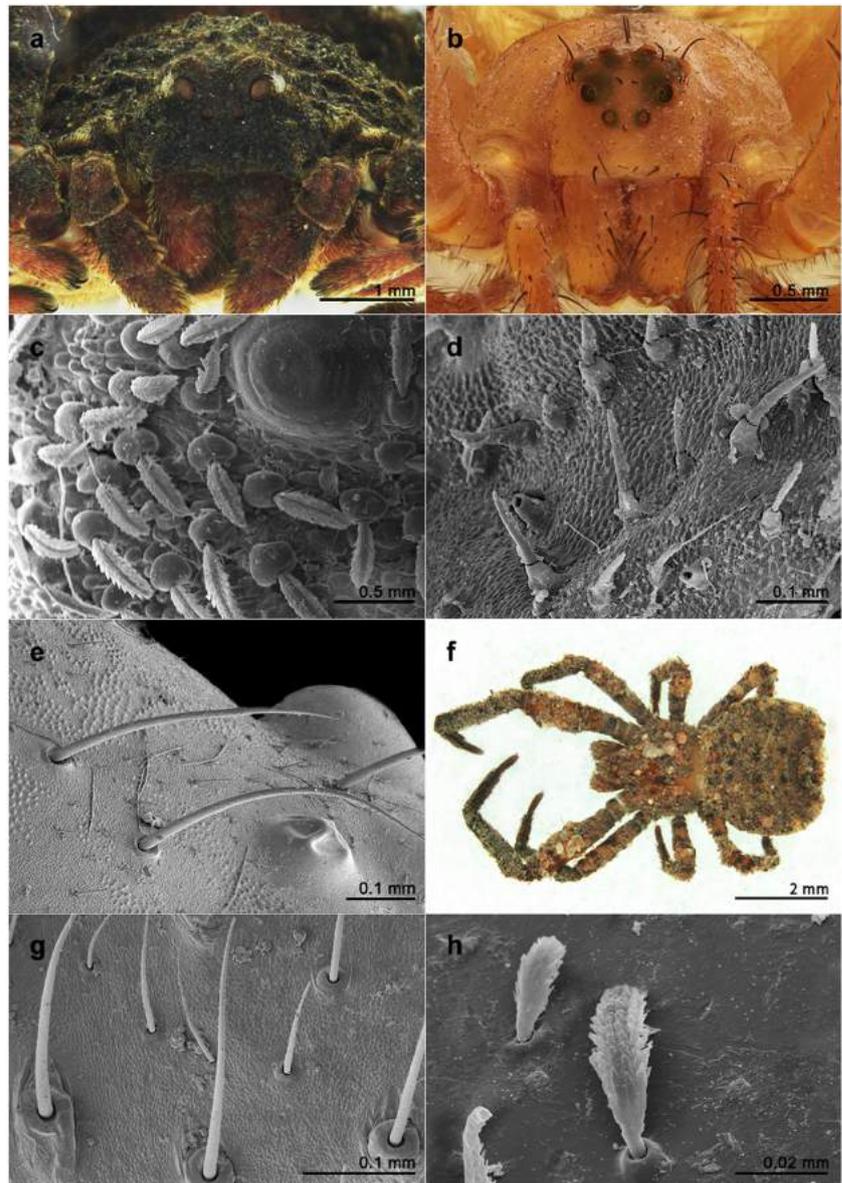
Fig. 9 Characters relative to carapace and sternum of specimens sampled in the present analysis: **a** *Sidymella bicuspidata*, sternum. **b** *Epicadus caudatus*, sternum. **c** *Onocolus intermedius*, sternum. **d** *Geraesta hirta* (white arrows indicate pointed setae; black arrows indicate filamentous setae). **e** *Sidymella trapezia*, sternum. f *Phrynarachne ceylonica*, sternum. **g** *Stephanopis macrostyla*, prosoma. **h** *Isala cambridgei* **comb. nov.**, prosoma
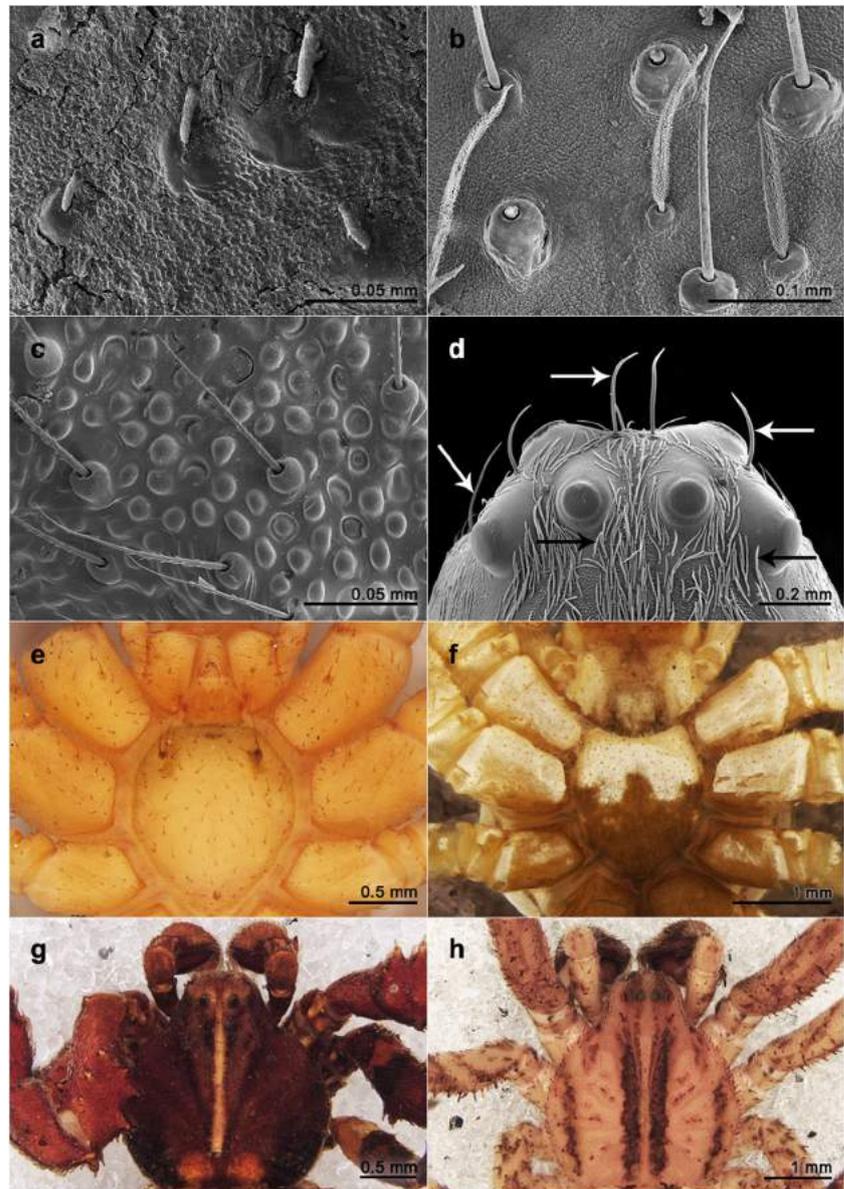
Fig. 10 Characters relative to prosoma of specimens sampled in the present analysis: **a** *Epicadus caudatus*, frontal view. **b** *Epicadus heterogaster*, carapace. **c** *Epicadus taczanowskii*, frontal view. **d** *Sidymella bicuspidata*. **e** *Tmarus elongatus*, lateral view. **f** *Epicadus heterogaster*, lateral view. **g** *Stephanopis nana*, frontal view (black arrows indicate lateral cephalic tubercles; white arrows indicate the not projected lateral margin of the clypeus). **h** *Epicadus rubripes*, frontal view (arrows indicate the lateral margins of the clypeus projected laterally)
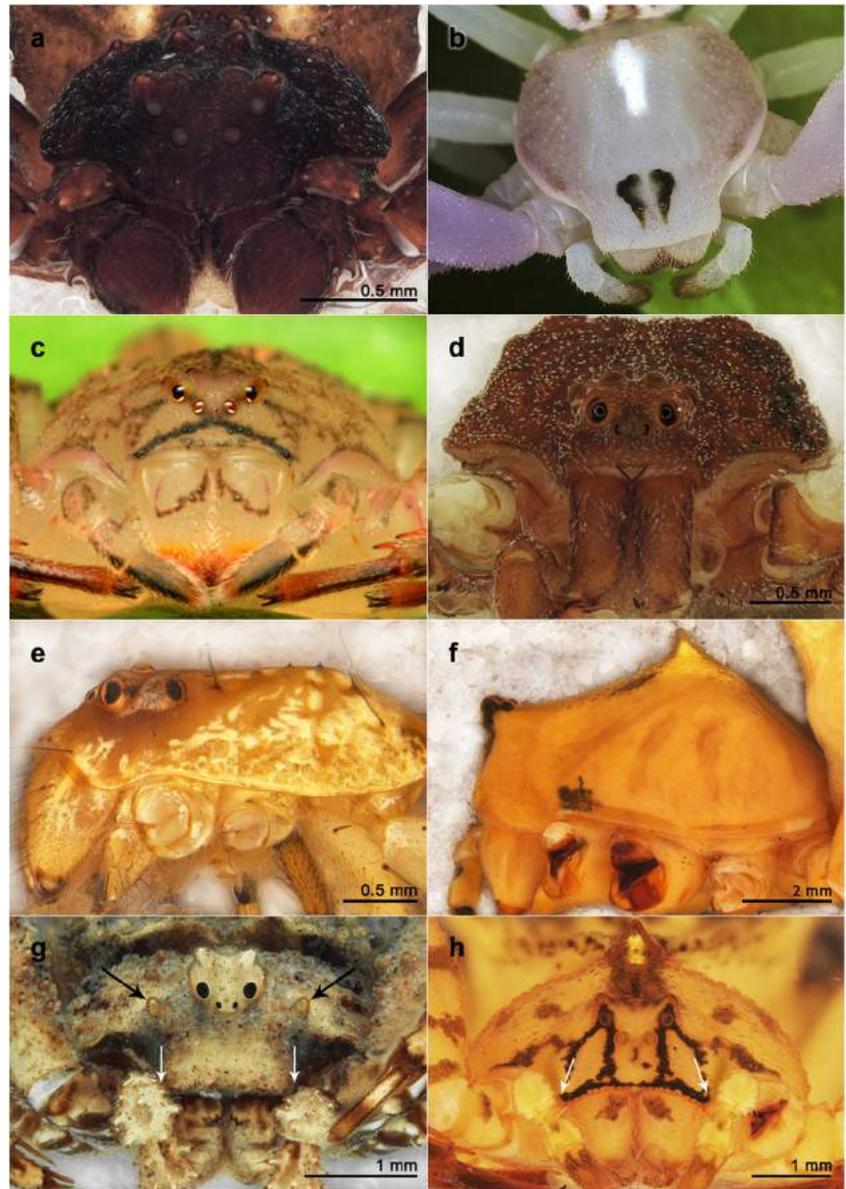
Fig. 11 Characters relative to prosoma and mouth parts of specimens sampled in the present analysis: **a** *Stephanopis monulfi*, frontal view. **b** *Sidymella* sp. 2, frontal view. **c** *Stephanopis quinquetuberculata*, lateral view. **d** *Stephanopis pentacantha*, **e** *Epicadus taczanowskii*, chelicerae (detail of papules). **f** *Stephanopoides simoni*, chelicerae. **g** *Phrynarachne ceylonica*, chelicerae. **h** *Epicadus trituberculatus*, chelicerae
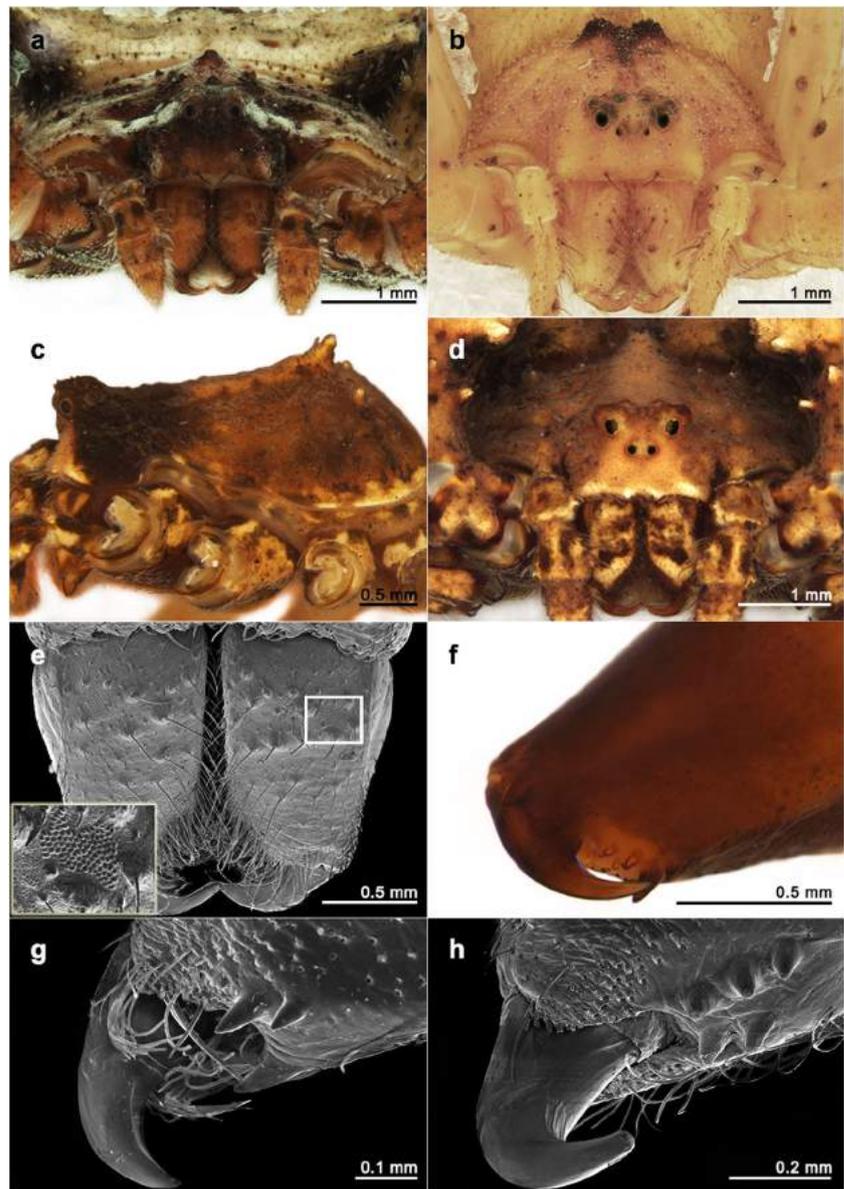
Fig. 12 Characters relative to carapace and mouth parts of specimens sampled in the present analysis: **a** *Borboropactus cinerascens*, labium and endites. **b** *Sidymella kolpogaster*, labium and endites. **c** *Tmarus elongatus*, frontal view. **d** *Stephanopis altifrons*, lateral view. **e** *Isala rufiventris* **comb. nov.**, frontal view (arrows indicate cheliceral macrosetae). **f** *Borboropactus cinerascens*, frontal view. **g** *Stephanopis barbipes*, frontal view. **h** *Stephanopis. bicornis*, frontal view
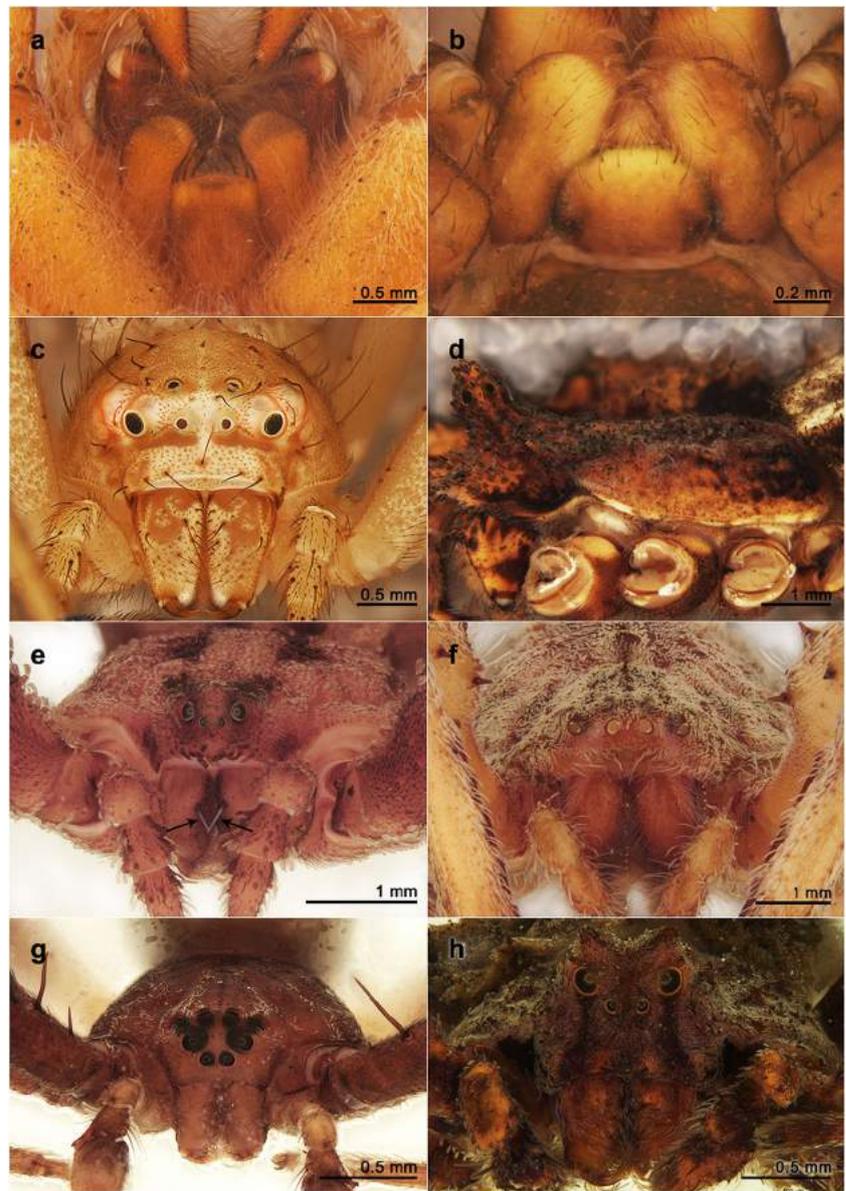
Fig. 13 Characters relative to carapace and legs of specimens sampled in the present analysis: **a** *Stephanopis pentacantha*, prosoma (detail of the procurve posterior eye row). **b** *Paratobias championi* **sp. rev.** (detail of the recurve posterior eye row). **c** *Stephanopis fissifrons*, prosoma (detail of the straight posterior eye row). **d** *Stephanopis barbipes*, prosoma (arrows indicate MOQ macrosetae). **e** *Borporopactus cinerascens*, prosoma (canoe-shaped tapetum). **f** *Tmarus elongatus*, tibiae I (trichobothria linearly distributed). **g** *Stephanopis pentacantha*, tibiae I (clustered trichobothria). **h** *Coenypha edwardsi*, leg I (arrows indicate mesial and ectal apophysis on femur)
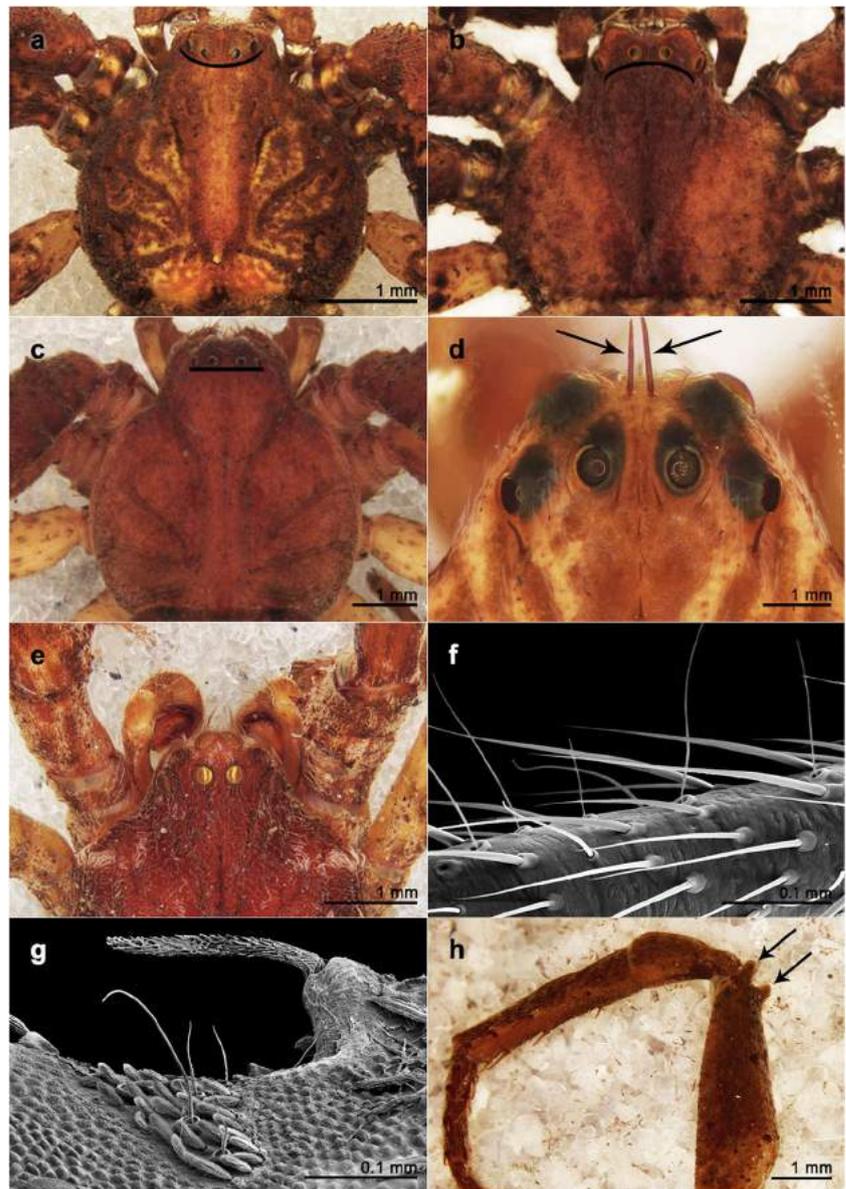
Fig. 14 Characters relative to legs of specimens sampled in the present analysis: **a** *Sidymella kolpogaster* (arrows indicate femoral setae). **b** *Sidymella trapezia* (arrow indicates femoral setae). **c** *Stephanopis monulfi*, leg I. **d** *Stephanopis lata*, leg I. **e** *Epicadus heterogaster*, femoral setiferous tubercles. **f** *Epicadus caudatus*, femoral setiferous tubercles. **g** *Geraesta hirta*, leg I. **h** *Stephanopis pentacantha*, leg I
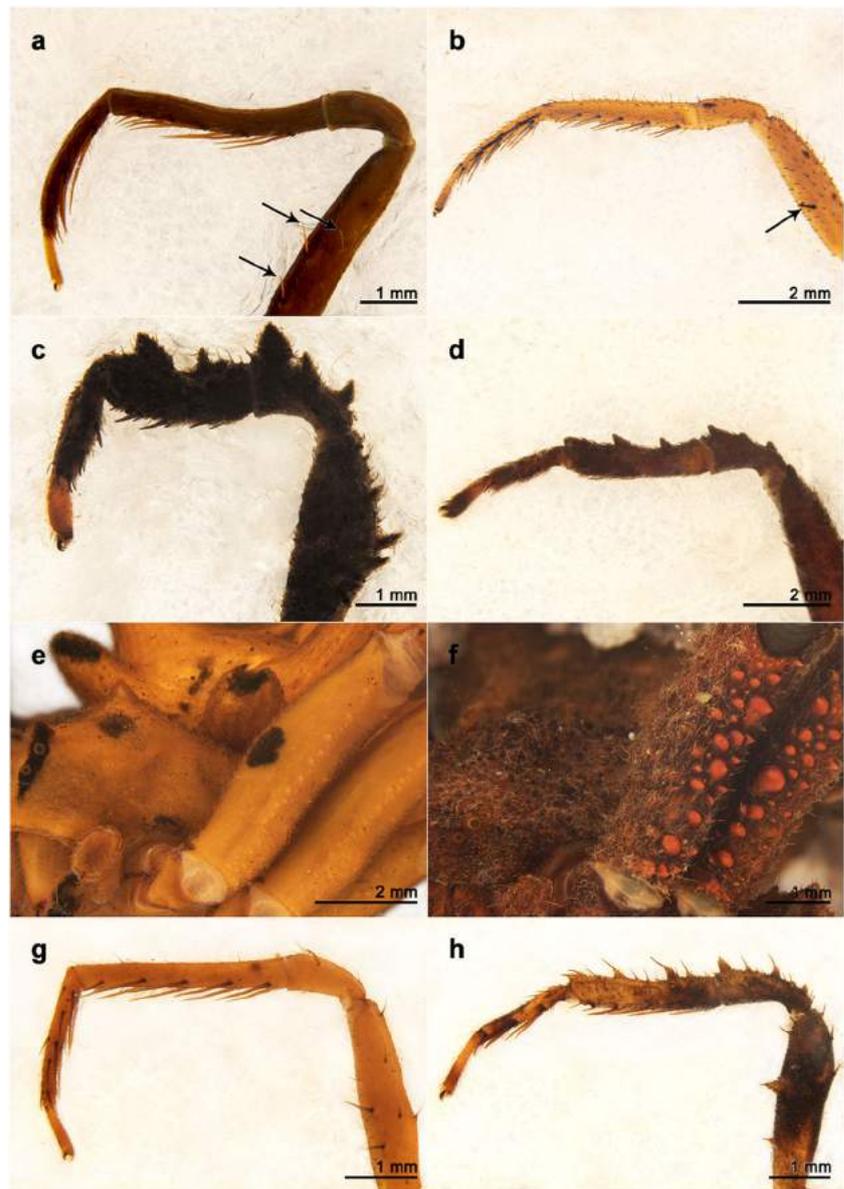
Fig. 15 Characters relative to legs, claws and opisthosoma of specimens sampled in the present analysis: **a** *Epicadus heterogaster*, patella I. **b** *Stephanopis pentacantha*, patella I. **c** *Isala cambridgei* **comb. nov.**, male tibial brushes. **d** *Epicadus caudatus*, trichobothrium and duster-shaped setae. **e** *Tmarus elongatus*, tarsal claws of the right leg I (mesial view). **f** *Epicadus taczanowskii*, tarsal claws of the right leg I (ectal view). **g** *Epicadus heterogaster*, tibia I. **h** *Epicadus trituberculatus*, opisthosoma
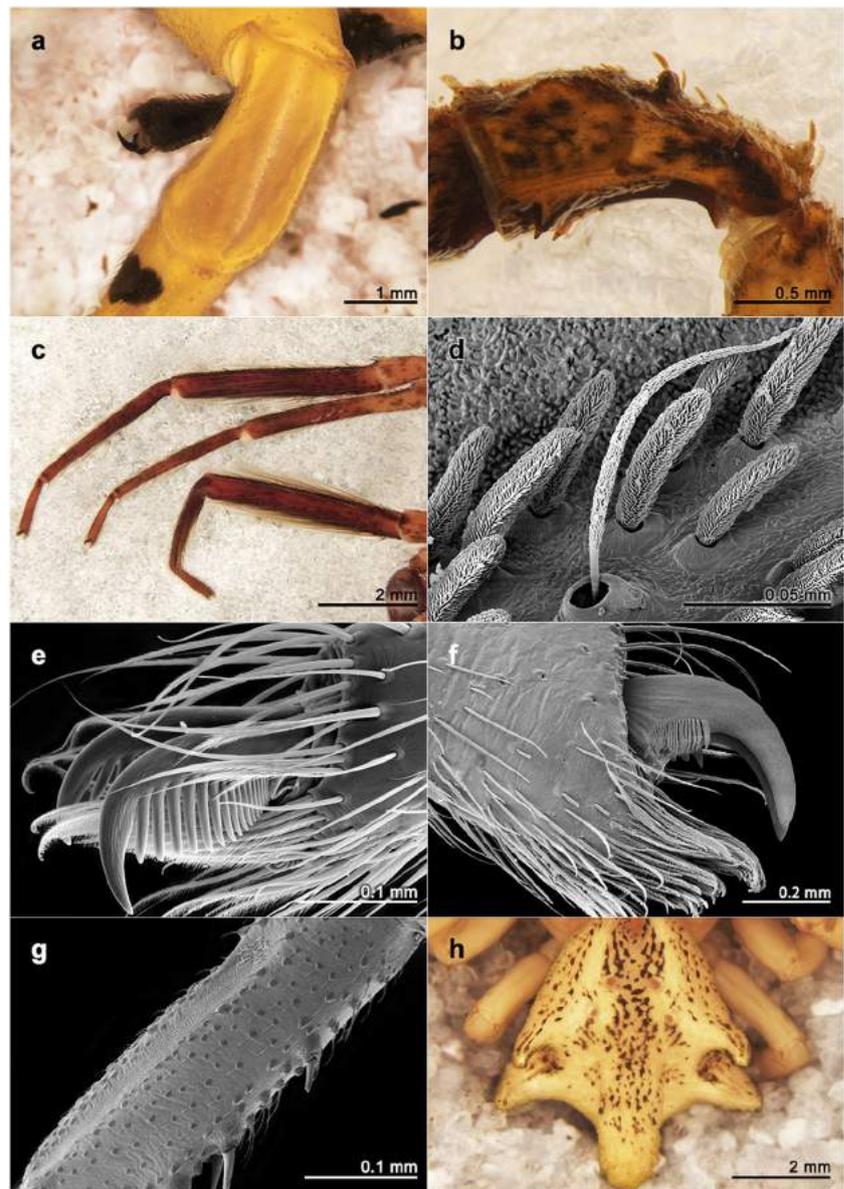
Fig. 16 Characters relative to opisthosoma of specimens sampled in the present analysis: **a** *Stephanopis nana*. **b** *Stephanopis monulfi*. **c** *Sidymella hirsuta*, **d** *Stephanopis altifrons*, cuspidate surface. **e** *Tmarus elongatus*, mazed-surface. **f** *Isala rufiventris* **comb. nov.**, granular surface. **g** *Isala punctata* **comb. nov.**, fingerprint surface. **h** *Sidymella hirsuta*, needle-shaped and filamentous setae
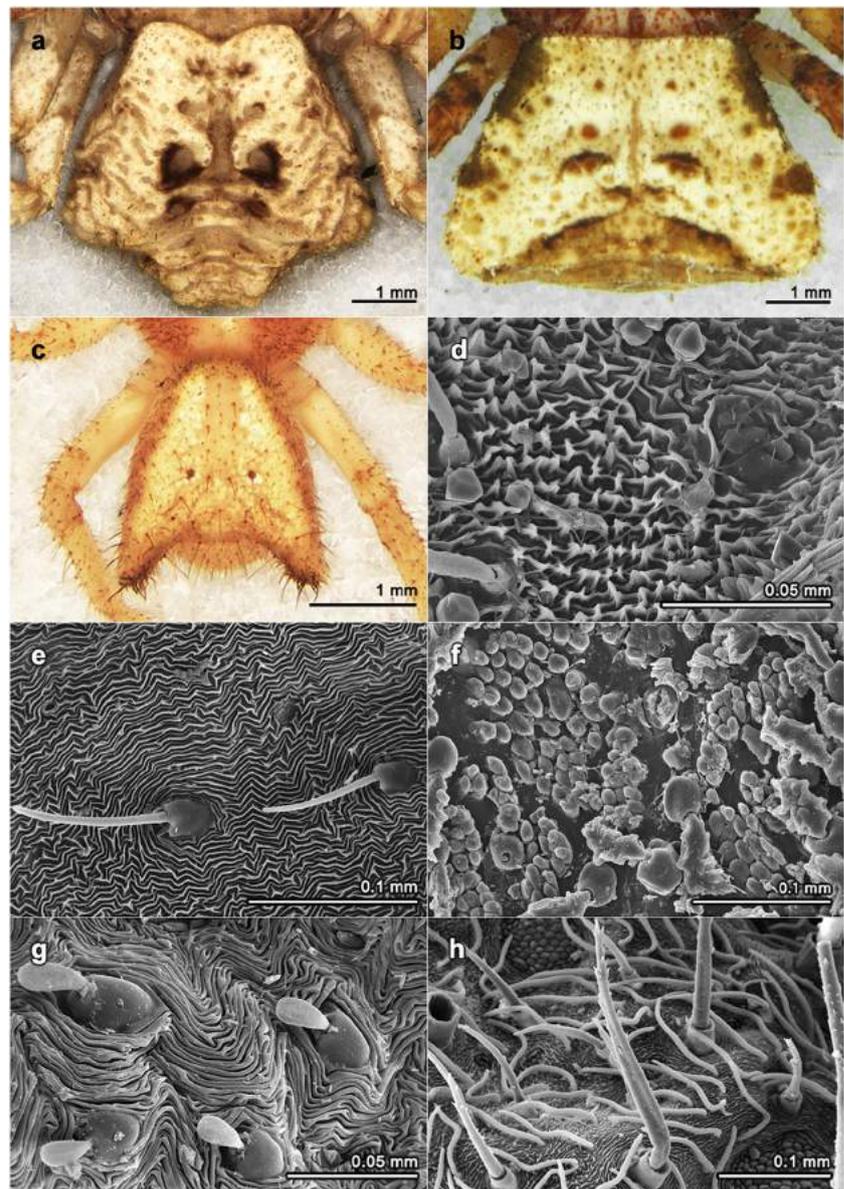
Fig. 17 Characters relative to opisthosoma and female genitalia of specimens sampled in the present analysis: **a** *Stephanopis lata* (arrows indicate abdominal setae clusters). **b** *Stephanopis monulfi*, barbed setae. **c** *Stephanopis monulfi*, ventral view of the epigynal plate. **d** *Coenypha antennata* **comb. nov.**, ventral view of the epigynal plate. **e** *Sidymella hirsuta*, dorsal view of the epigynal plate (arrows indicate the direction of entry into the copulatory ducts). **f** *Coenypha antennata* **comb. nov.**, dorsal view of the epigynal plate (arrows indicate the direction of entry into the copulatory ducts). **g** *Sidymella* sp.1, dorsal view of the epigynal plate. **h** *Epicadus trituberculatus*, dorsal view of the epigynal plate
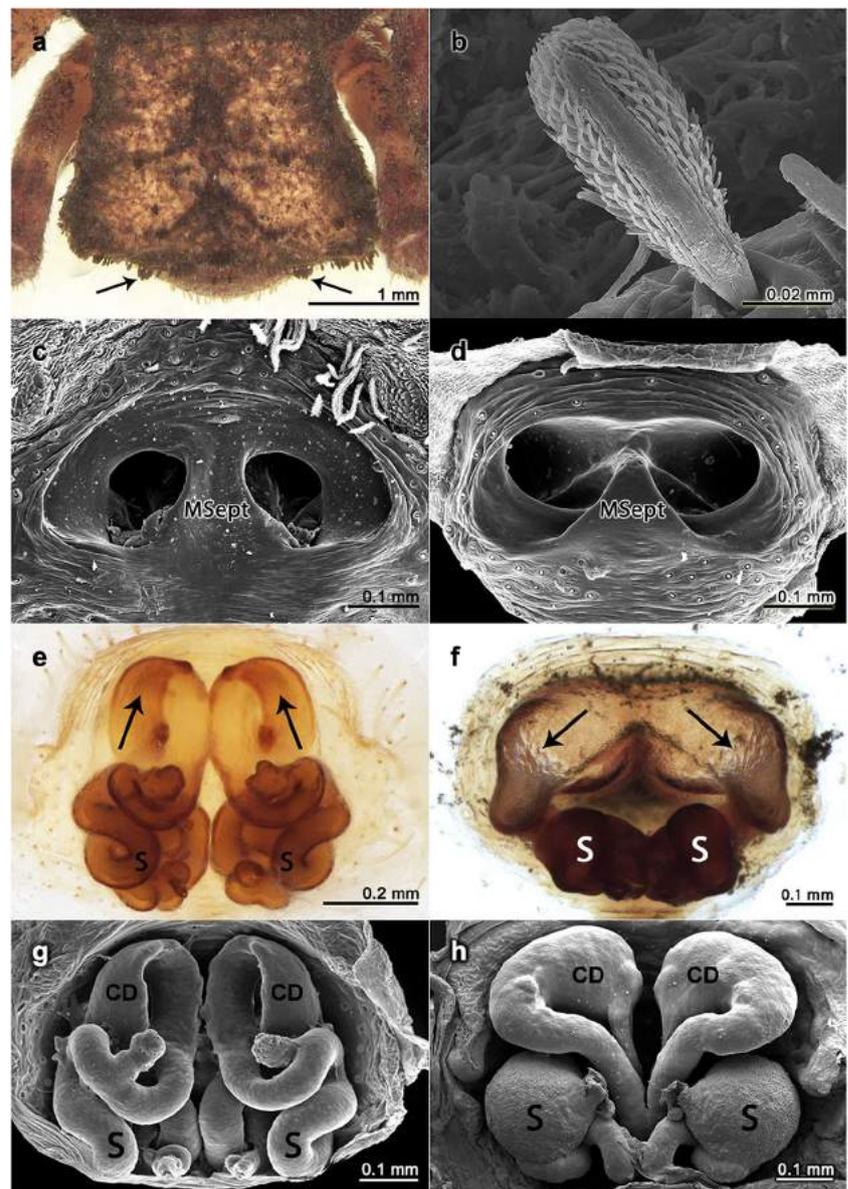
Fig. 18 Characters relative to the female and male genitalia of specimens sampled in the present analysis: **a** *Isala spiralis* **comb. nov.**, dorsal view of the epigynal plate. **b** *Stephanopis armata*, dorsal view of the epigynal plate. **c** *Paratobias championi* **sp. rev.**, ventral view of the epigynal plate. **d** *Coenypha nodosa* **comb. nov.**, ventral view of the epigynal plate. **e** *Stephanopis lata*, ventral view of the epigynal plate. **f** *Borboropactus cinerascens*, ventral view of the epigynal plate (arrows indicate the epigynal teeth). **g** *Stephanopis flagellata*, left palp. **h** *Sidymella bicuspidata*, left palp
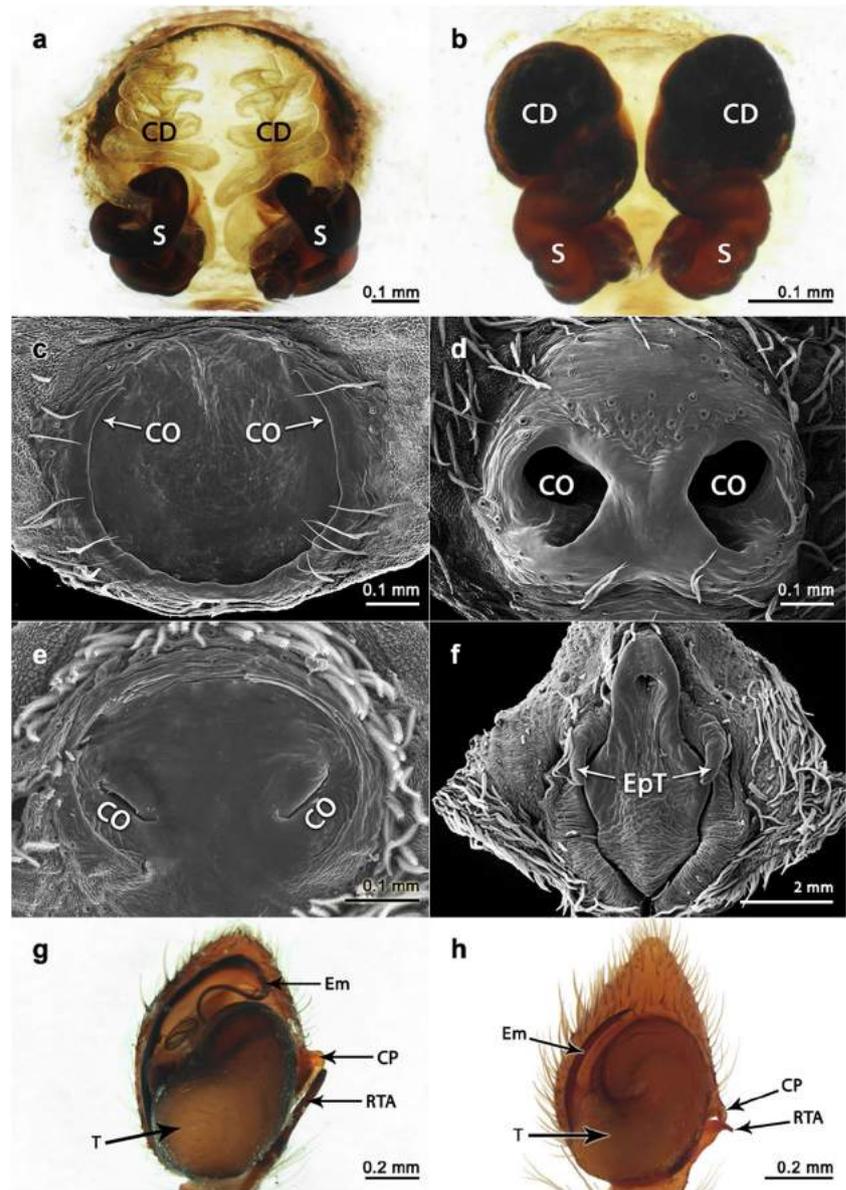
Fig. 19 Characters relative to the male genitalia of specimens sampled in the present analysis: **a** *Epicadus trituberculatus*, left palp. **b** *Stephanopis pentacantha*, left palp (arrow indicates the prolateral macrosetae). **c** *Geraesta hirta*, left palp. **d** *Sidymella lucida*, retrolateral view of left palp. **e** *Borboropactus nyerere*, left palp. **f** *Isala cambridgei* **comb. nov.**, retrolateral view of left palp. **g** *Stephanopis nigra*, retrolateral view of left palp. **h** *Stephanopis altifrons*, detail of the RTA
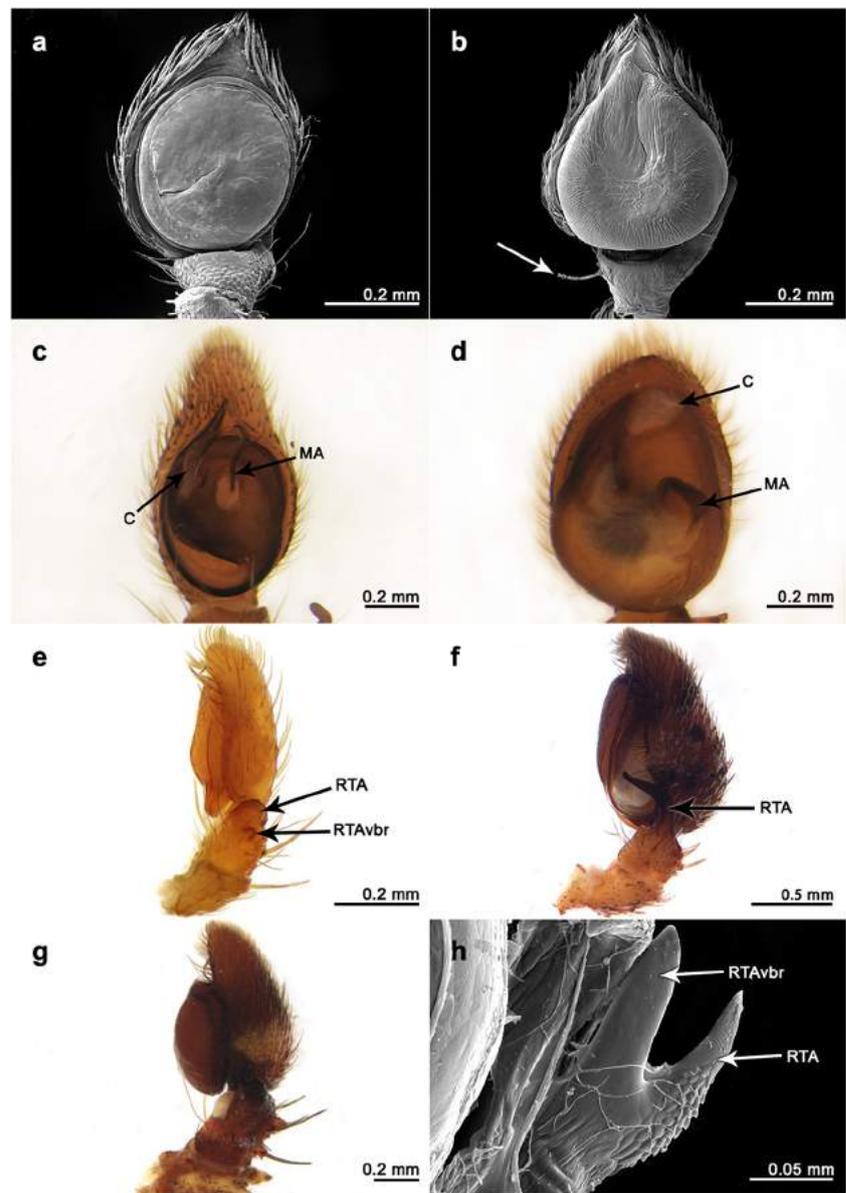
Fig. 20 Characters relative to the male genitalia of specimens sampled in the present analysis: **a** *Stephanopis fissifrons*, grooved RTA. **b** *Sidymella lucida*, nodose RTA. **c** *Isala palliolata* **comb. nov.**, smooth RTA. **d** *Epicadus taczanowskii*, canoe-shaped RTAbvr. **e** *Sidymella hirsuta*, spoon-shaped RTAvbr. **f** *Coenypha ditissima* **comb. nov.**, left palp. **g** *Sidymella furcillata*, left palp. **h** *Isala spiralis* **comb. nov.**, left palp
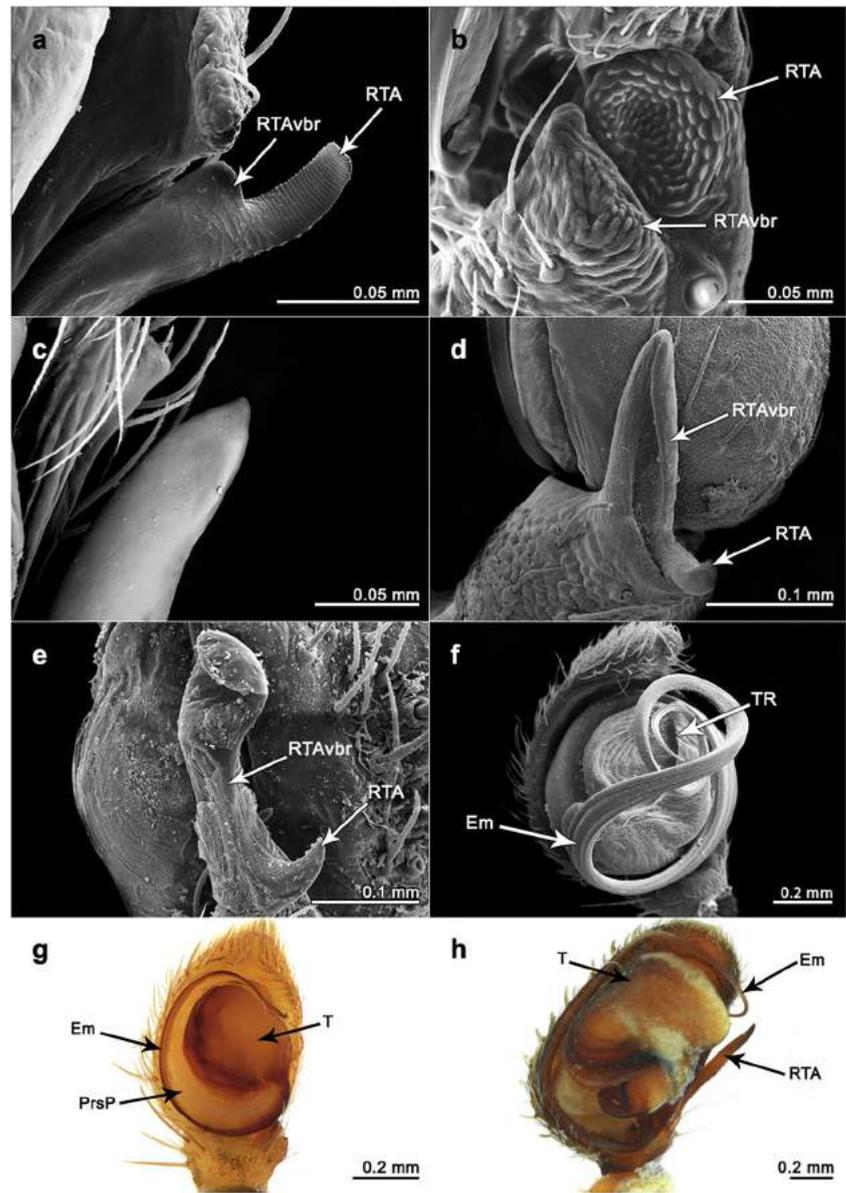
Fig. 21 Characters relative to the male genitalia of specimens sampled in the present analysis: **a** *Stephanopis barbipes*, left palp. **b** *Isala cambridgei* **comb. nov.**, left palp. **c** *Onocolus intermedius*, left palp. **d** *Sidymella longispina*, left palp. **e** *Paratobias* sp. 1, left palp. **f** *Tmarus polyandrus*, left palp. **g** *Stephanopis altifrons*, left palp (lower arrows indicate the pair of ventral filamentous setae on tibiae). **h** *Stephanopis bicornis*, retrolateral view of left palp (detail of the cymbial setae brush)
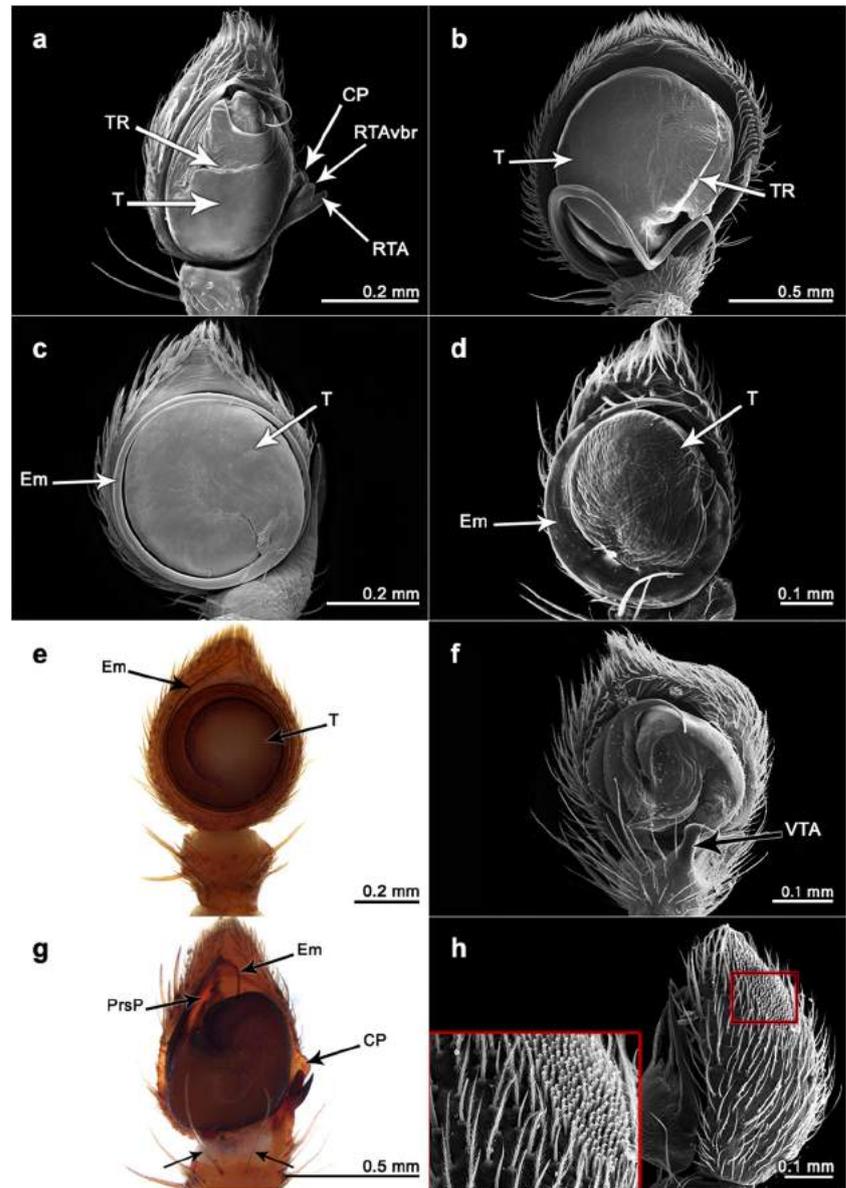
References

Benjamin, S. P. (2011). Phylogenetics and comparative morphology of crab spiders (Araneae: Dionycha, Thomisidae). *Zootaxa, 3080*, 1–108.

Benjamin, S. P. (2013). On the crab spider genus *Angaeus* Thorell, 1881 and its junior synonym *Paraborboropactus* Tang and Li, 2009 (Araneae: Thomisidae). *Zootaxa, 3636*, 71–80.

Benjamin, S. P. (2015). On the African crab spider genus *Geraesta* Simon, 1889 (Araneae: Thomisidae). *African Invertebrates, 56*, 309–318.

Benjamin, S. P. (2016). Revision of *Cebrenninus* Simon, 1887 with description of one new genus and six new species (Araneae: Thomisidae). *Revue Suisse Zoologie, 123*, 179–200.

Benjamin, S. P. (2017). A new species of *Angaeus* from Malaysia with possible affinity to related genera within Stephanopinae (Araneae: Thomisidae). *Zootaxa, 4337*, 297–300.

Benjamin, S. P., Dimitrov, D., Gillespie, R. G., & Hormiga, G. (2008). Family ties: molecular phylogeny of crab spiders (Araneae: Thomisidae). *Cladistics, 24*, 708–722.

Bradley, H. B. (1871). Descriptions of eight new species of *Stephanopis* (Cambridge). *Transactions of the Entomological Society of New South Wales, 2*, 233–238.

Bryant, E.B. (1933). Notes on types of Urquhart's spiders. Records of the Canterbury Museum, 4, 1–27.

Dias, S. C., & Brescovit, A. D. (2003). Notes on the behavior of *Pachistopelma rufonigrum* Pocock (Araneae, Theraphosidae, Aviculariinae). *Revista Brasileira de Zoologia, 20*, 13–17.

Gawryszewski, F. M. (2014). Evidence suggests that modified setae of the crab spiders *Stephanopis* spp. fasten debris from the background. *Zoomorphology, 133*, 205–215.

Goldsbrough, C., Hochuli, D., & Shine, R. (2004). Fitness benefits of retreat-site selection: spiders, rocks, and thermal cues. *Ecology, 85*, 1635–1641.

Goloboff, P. (1999). Analyzing large data sets in reasonable times: solutions for composite optima. *Cladistics, 15*, 415–428.

Goloboff, P., & Farris, J. (2001). Methods for quick consensus estimation. *Cladistics, 17*, S26–S34.

Goloboff, P. A., Carpenter, J. M., Arias, J. S., & Miranda-Esquivel, D. R. (2008b). Weighting against homoplasy improves phylogenetic analysis of morphological data sets. *Cladistics, 24*, 758–773.

Goloboff, P. A., Farris, J. S., Källersjö, M., Oxelman, B., Ramírez, M., & Szumik, C. A. (2003). Improvements to resampling measures of group support. *Cladistics, 19*, 324–332.

Goloboff, P. A., Farris, J. S., & Nixon, K. C. (2008a). TNT, a free program for phylogenetic analysis. *Cladistics, 24*, 774–786.

Goloboff, P. A., Galvis, A. T., & Arias, J. S. (2018a). Parsimony and model-based phylogenetic methods for morphological data: comments on O'Reilly et al. *Palaeontology, 61*, 625–630.

Goloboff, P. A., Torres, A., & Arias, S. (2018b). Weighted parsimony outperforms other methods of phylogenetic inference under models appropriate for morphology. *Cladistics, 34*, 407–437.

Koch, L. (1874). *Die Arachniden Australiens*. Nürnberg, DE: Verlag von Bauer & Raspe.

Lise, A.A. (1973). Contribuição ao conhecimento do gênero Sidyma no Brasil, com descrição de uma nova espécie (Araneae-Thomisidae). *Iheringia, 43*, 3–47.

Machado, M., Teixeira, R. A., & Lise, A. A. (2015). Taxonomic notes on the crab spider genus *Tobias* Simon, 1895 (Araneae, Thomisidae, Stephanopinae). *Zootaxa, 4034*, 565–576.

Machado, M., Teixeira, R. A., & Lise, A. A. (2017). Cladistic analysis supports the monophyly of the Neotropical crab spider genus *Epicadus* and its senior synonymy over *Tobias* (Araneae: Thomisidae). *Invertebrate Systematics, 31*, 442–455.

Machado, M., Teixeira, R. A., & Lise, A. A. (2018). There and back again: more on the taxonomy of the crab spider genus *Epicadus* (Thomisidae: Stephanopinae). *Zootaxa, 4382*, 501–530.

Machado, M., Guzati, C., Viecelli, R., Molina-Gómez, D., & Teixeira, R. A. (2019a). A taxonomic review of the crab spider genus Sidymella (Araneae, Thomisidae) in the Neotropics. *Zoosystematics and. Evolution, 95*, 319–344.

Machado, M., Teixeira, R. A., & Milledge, G. A. (2019b). On the Australian bark crab spiders genus Stephanopis: taxonomic review and description of seven new species (Araneae: Thomisidae: Stephanopinae). *Records of the Australian Museum, 71*, 217–276.

Mello-Leitão, C. F. (1929). *Aphantochilidas e Thomisidas do Brasil*. Rio de Janeiro, BR: Archivos do Museu Nacional.

Mirande, J. M. (2009). Weighted parsimony phylogeny of the family Characidae (Teleostei: Characiformes). *Cladistics, 25*, 574–613.

Morrone, J. J. (1994). Distributional patterns of Rhytirrhinini (Coleoptera: Curculionidae) and the historical relationships of the Andean provinces. *Global Ecology and Biogeography Letters, 4*, 188–194.

Morrone, J. J. (2014). Biogeographical regionalisation of the Neotropical region. *Zootaxa, 3782*, 1–110.

Morrone, J. J. (2015). Biogeographical regionalisation of the Andean region. *Zootaxa, 3936*, 207–236.

Nixon, K. C. (1999). The Parsimony Ratchet, a new method for rapid parsimony analysis. *Cladistics, 15*, 407–414.

O'Reilly, J., Puttick, M. N., Pisani, D., & Donoghue, P. C. J. (2018). Probabilistic methods surpass parsimony when assessing clade support in phylogenetic analyses of discrete morphological data. *Paleaontology, 61*, 105–118.

Pickard-Cambridge, O. (1869). Descriptions and sketches of some new species of Araneida, with characters of a new genus. *Annals and Magazine of Natural History, 3*, 52–74.

Prado, A. W., Baptista, R. L. C., & Machado, M. (2018). Taxonomic review of *Epicadinus* Simon, 1895 (Araneae: Thomisidae). *Zootaxa, 4459*, 201–234.

Puttick, M. N., O'Reilly, J. E., Pisani, D., & Donoghue, P. C. J. (2019). Probabilistic methods outperform parsimony in the phylogenetic analysis of data simulated without a probabilistic model. *Palaeontology, 62*, 1–17.

Rambaut, A., Drummond, A. J., Xie, D., Baele, G., & Suchard, M. A. (2018). Posterior summarisation in Bayesian phylogenetics using Tracer 1.7. *Systematic Biology, 5*, 901–904.

Ramírez, M. J. (2014). The morphology and phylogeny of dionychan spiders (Araneae: Araneomorphae). *Bulletin of the American Museum of Natural History, 390*, 1–374.

Ronquist, F., Teslenko, M., Van Der Mark, P., Ayres, D. L., Darling, A., Höhna, S., et al. (2012). Mrbayes 3.2: efficient bayesian phylogenetic inference and model choice across a large model space. *Systematic Biology, 61*, 539–542.

Silva-Moreira, T., & Machado, M. (2016). Taxonomic revision of the crab spider genus *Epicadus* Simon, 1895 (Arachnida: Araneae: Thomisidae) with notes on related genera of Stephanopinae Simon, 1895. *Zootaxa, 4147*, 281–310.

Simon, E. (1895). *Histoire naturelle des araignées*. Paris, FR: Librairie Encyclopédique de Roret.

Simon, E. (1903). *Histoire naturelle des araignées*. Paris, FR: Librairie Encyclopédique de Roret.

Sirvid, P. J., Moore, N. E., Chambers, G. K., & Prendergast, K. (2013). A preliminary molecular analysis of phylogenetic and biogeographic relationships of New Zealand Thomisidae (Araneae) using a multi-locus approach. *Invertebrate Systematics, 27*, 655–672.

Smith, M. R. (2019). Bayesian and parsimony approaches reconstruct informative trees from simulated morphological datasets. *Biological Letters, 15*, 20180632.

Teixeira, R. A., Campos, L. A., & Lise, A. A. (2014). Philogeny of Aphantochilinae and Strophinae sensu Simon (Araneae; Thomisidae). *Zoologica Scripta, 43*, 65–78.

Weiler, L., Ferrari, A., & Grazia, J. (2016). Phylogeny and biogeography of the South American subgenus *Euschistus* (*Lycipta*) Stål (Heteroptera: Pentatomidae: Carpocorini). *Insect Systematics and Evolution, 47*, 313–346.

Wheeler, W. C., Coddington, J. A., Crowley, L. M., Dimitrov, D., Goloboff, P. A., Griswold, C. E., Hormiga, G., Prendini, L., Ramírez, M. J., Sierwald, P., Almeida-Silva, L., Alvarez-Padilla, F., Arnedo, M. A., Benavides Silva, L. R., Benjamin, S. P., Bond, J. E., Grismado, C. J., Hasan, E., Hedin, M., Izquierdo, M. A., Labarque, F. M., Ledford, J., Lopardo, L., Maddison, W. P., Miller, J. A., Piacentini, L. N., Platnick, N. I., Polotow, D., Silva-Dávila, D., Scharff, N., Szűts, T., Ubick, D., Vink, C. J., Wood, H. M., & Zhang, J. (2017). The spider tree of life: phylogeny of Araneae based on target-gene analyses from an extensive taxon sampling. *Cladistics, 33*, 574–616.

Maddison, W.P. & Maddison, D.R. (2019). Mesquite: a modular system for evolutionary analysis. Version 3.6. http://mesquiteproject.org. Accessed 18 November 2019.

Nixon, K. C. (1999–2004). Winclada (BETA) ver. Asado 1.89. http://www.cladistics.com/about_winc.htm. Accessed 20 March 2014.

World Spider Catalog. (2020). World Spider Catalog version 21.0. Natural History Museum Bern. http://wsc.nmbe.ch. Accessed 02 June 2020.